Master of Science Thesis

Morphological impact of the Sinterklaas storm at Het Zwin

Numerical modelling with XBeach

B. I. Carrión Aretxabala

TU Delft Delft University of Technology

Deltares Enabling Delta Life

Challenge the future

Front cover: aerial photography of the mouth of Het Zwin—its most active morphological area. The tidal channel crosses the dune rows and roughly divides The Netherlands from Belgium. Behind the Dutch dikes the city of Cadzand is also visible. Picture from the Rijkswaterstaat Image Archive, available at https://beeldbank.rws.nl/Photos/2855/428285.jpg.

Morphological impact of the Sinterklaas storm at Het Zwin

Numerical modelling with XBeach

by

B. I. Carrión Aretxabala

in partial fulfillment of the requirements for the degree of

Master of Science
in Civil Engineering

at the Delft University of Technology,
to be defended publicly on Monday May 18, 2015 at 15:00
in lecture room D of the Civil Engineering building.

Thesis committee	Prof. dr. ir. M. J. F. Stive	TU Delft	
	Prof. dr. ir. A. J. H. M. Reniers	TU Delft	– Deltares
	Ir. A. A. van Rooijen	Deltares	– TU Delft
	Dr. ir. M. Boers	Deltares	
	Ir. P. L. M. de Vet	TU Delft	– Deltares

TU Delft Delft University of Technology

Deltares Enabling Delta Life

Para Magdalena y Arturo

Preface

The writing of this report—and its defence—marks the end of my studies at Delft Technology University, pursuing a Master of Science degree. It has been a little less than two years living in the kid-friendly, efficient and tolerant country of The Netherlands, in the lovely little town of Delft. For sure, it has been a nice change for me and my family coming from the ever-rushing Santiago de Chile, and certainly we'll miss the quiet ambience of this "human scale" city. I must say I owe Holland a great deal—the time for raising our daughter, who arrived as a baby and now leaves as a happy and confident little girl along with is new-born brother, will be landmarks in the history of our family.

I am honoured for having had the chance to meet and interact with so many talented academics and professionals, many of them leaders on the field of Coastal Engineering. It is no mystery that both TU Delft and Deltares are world-class institutions and I'm nothing but grateful for the intense time I have spent here. I humbly feel that I have learned new things and now I have a broader and more mature view on the coastal processes and the ways we have to understand and engineer them.

Of course I couldn't be writing this note without the support of many people, which I'd like to acknowledge here. First of all I'd like to thank my company, PRDW, for their continuous support and particularly Javier Vásquez for his smart and close leadership—he's been an important mentor in my professional career. A big thanks also to the millions of Chilean tax-payers who have economically supported us these years, via the government scholarship programme "Becas Chile". Concerning the development of this thesis I'd like to recognize the useful insights and recommendations made by TU Delft professors Ad Reniers and Marcel Stive, who were kind enough to listen to my problems and ideas. From Deltares I'd like to thank Marien Boers and Lodewijk de Vet who where always willing to discuss and help me with their knowledge and experience, which (I hope) enriched the work I've done. To Joost den Bienman I owe profiting the Linux cluster which allowed me to perform parallel runs and save me a big deal of time, and to Robert McCall I'm grateful for the interesting and challenging conversations we had about the details of the XBeach model. Especially I'd like to thank Arnold van Rooijen, who was committed to the success of this thesis from the beginning. Without his help and continuous interest this work would have been much harsher to do.

Finally, but most importantly, I have to thank my wife Leticia who supported the idea of coming abroad from (almost) the very beginning. It's actually a funny story: I told her about the possibility of travelling to Holland for a couple of years the week after we moved to our new apartment—the last moving we were expecting to do in a while—which coincided with the week after our daughter was born. So she wasn't all for it at that exhausting moment. However, as she has always done, she backed me up in this project and actually now she wouldn't leave The Netherlands if we had the choice! Jokes apart, she has always been my strongest support and if I had accomplished anything, it's been by a large degree thanks to her, so many thanks again to my best friend and lovely wife.

B. I. Carrión Aretxabala
Delft, April 2015

Summary

A very large storm hit the coasts of The Netherlands—and most of north-west Europe—during the evening of the 5th of December 2013. The *Sinterklaas storm*, as it was later known, induced extremely high water levels and substantial dune erosion all along the Dutch coastline. In this thesis the morphological impact of the Sinterklaas storm at one particular location—Het Zwin—will be analysed from measurements and simulated with the process-based model XBeach.

Het Zwin is a relatively small natural reserve shared between The Netherlands and Belgium. It is a brackish reservoir dominated by the tide, composed mainly by tidal flats protected from the sea by beach dunes and separated from the hinterland by clay dikes. Actually it is hard to classify the Zwin; it is not really an estuary, given its small dimensions, nor a tidal inlet since no lagoon is present behind the dunes. Probably it is best defined by the Dutch word "slufter".

Two different storm regimes were observed at Het Zwin during the Sinterklaas storm: dune erosion (collision), and storm overwash, the latter confined at a precise location where the Dutch dunes were lower and narrower. The storm impact was deduced from lidar measurements of the terrain elevation prior and after the event, and the hydrodynamic conditions of the storm were obtained from wave buoys and tide gauges deployed and maintained by both countries.

These data were used as inputs for a numerical hind-cast of the storm impact. Calibration of the model considered sensitive parameters that were either meaningful physical inputs, such as the bottom friction, or numerical proxies for physical processes, such as the critical slope for avalanching. As suggested in previous studies, the collision regime was found to be dependent on the onshore transport induced by short-waves, whereas the overwash regime and the washover fan were determined by the bottom friction at the higher parts of the dunes. The best fit was obtained with parameters `facua` $= 0.10$, and `C` $= 25$, respectively.

Additionally, the critical slope for avalanching which produced the best fit, both in sand loss and profile shape, was found to be `wetslp` $= 0.20$, slightly lower than the recommended default value of 0.30. However, it is argued that the actual value to be used in other studies might be a function of the grid size, since it determines the ability of the model to assess the terrain slope.

Morphodynamic numerical modelling is normally a costly task. For this particular site of study three factors induced very large simulation times, which rendered the modelling with XBeach *unworkable*:

- A rather large domain is needed to incorporate the refraction of the wave data.
- A very fine grid is required in order to reproduce the flooding and drying processes of the overwash and (in a lesser way) the avalanching of the dunes' face.
- The duration of the storm, of a few days, is rather large compared with the physical events being modelled, which have a time scale of a fraction of seconds.

A central issue in this thesis is the optimization of the runtime of XBeach (and by extension, any other process-based numerical model). Two techniques are discussed and tested, which allowed the hind-cast to be computed in just over a day:

- The use of curvilinear over rectangular grids, in order to focus computational effort. The same precision can be obtained using fewer grid cells.
- The computation of the hydrodynamic forcing by waves and water levels only once, and later feed those results to a smaller dedicated grid to perform the morphodynamic computations. This is a straightforward offline coupling scheme.

The use of these techniques significantly reduce the computation effort without compromising the accuracy nor the reliability of the results.

Contents

List of Figures

List of Tables

1

Introduction

During the evening of the 5th of December 2013 one of the biggest storms in recent years hit The Netherlands and other countries in north-west Europe, causing floods and dune erosion along the coastlines. Particularly, the dunes around the tidal inlet of Het Zwin—located at the south-west of The Netherlands—suffered from scarping and overwash. The storm was well documented, and reliable measurements of the wind, waves, and water levels before, during and after the storm were available. Additionally, accurate measurements of the topography of the dunes were carried out before and after the event, from which a good estimate of the storm impact can be made.

Due to the limited spatial extent of the storm impact at Het Zwin combined with the small uncertainty in the inputs, this is a good field case for testing a process-based numerical model, such as *XBeach*. XBeach is event-driven morphological model, continuously being developed at Deltares (along with worldwide cooperation). It is a state of the art, free and open-source software, which includes all the relevant physics needed to model the morphological response of a sandy system to a storm event.

The morphological impact of the 2013 Sinterklaas storm at Het Zwin is an interesting case for testing XBeach for the following reasons:

- Het Zwin presents a complex area with high long-shore variability. The presence of a tidal channel is likely to induce highly three dimensional flow patterns, which might be challenging to reproduce by a vertically averaged model.
- Two distinguishable storm impact regimes were present at Het Zwin—dune overwash and collision—clearly separated by the tidal inlet, i.e. the Belgian side only presented dune erosion (collision), whereas only one localized overwash event occurred in the Dutch side.
- In contrast with some previous studies involving overwash, the quality of the measurement of this storm can be considered very high.

1.1. Problem description

Dunes are a critical component in the *dike ring*[1] safety scheme of The Netherlands in particular, and for any sandy coastal environment in general. Hence, it is of key importance to correctly evaluate their response to stormy events. Reliable safety assessment of the coastal areas is increasingly important as the world's population and economy grow and exert additional pressure on these fragile ecosystems.

Most tools currently employed by coastal managers are largely empirical and/or are not able to take into account alongshore variability. The direct consequence of this is the mis- or under-representation of physical processes, which might lead to unreliable results. Notably, the alongshore variations of topography have been indicated as a key element in producing accurate hind-cast and realistic forecasts of the impact of storms or hurricanes on sandy coasts.

[1] http://www.risicokaart.nl/en/informatie_over_risicos/overstroming/

Some more comprehensive alternatives comprise the use of process-based models, which incorporate more physical aspects. These models tend to be more robust and reliable, but also more expensive to run considering needed resources, time consumption, and required knowledge to operate them and interpret their results. These models are relatively new, and continuously under development.

1.2. Objective and research questions

The main objective of the thesis is to (further) validate XBeach as a storm impact assessment tool using data from the 2013 Sinterklaas storm measured at Het Zwin, The Netherlands. A particular objective is to investigate its ability to reproduce the overwash regime, which in principle should lie within the model capabilities but has presented difficulties in the past.

One interesting topic often neglected, or at least not often covered in the literature, is the runtime optimization for this kind of models. This tends to be considered a *practical* matter and, thus, not an intellectual exercise worthy of academic discussion. This subject, however, will be discussed in this report for two main reasons:

- The author *is* an engineer, whose habitual work is to deal with the practicalities of numerical models, the runtime being one of their critical aspects.
- The need for a workable runtime might lead to neglect, dismiss or distort relevant physical processes in the modelling, even unintentionally.

The runtime analysis is performed to question some commonly made assumptions in XBeach and shed light on their possible implications, along with proposing and testing alternatives to circumvent them.

The research questions that motivate this work can be listed as:

- What are the physical processes that dominate the morphological impact during a severe storm?
- How do these processes differ between the different storm impact regimes—dune erosion/collision and overwash?
- Is XBeach able to reproduce both regimes observed at Het Zwin? Particularly, is XBeach able to reproduce the storm overwash observed at the Dutch part of Het Zwin?
- What is the best set of model parameters and how do they compare with the default set, and those used in similar literature studies?

Concerning the coastal management of Het Zwin, the following question arise:

- What would have been the impact should the storm conditions have been more severe?
- How does the position of the tidal channel influences the storm impact over the Dutch dunes?

The focus of this thesis will be on the short-term impact, hence the long-term morphodynamics of Het Zwin, and error analysis of the inputs will remain explicitly our of the scope of this thesis.

1.3. Outline of the report

This thesis report is organized as follows. A background chapter (2) covers the descriptions of the physical system of Het Zwin estuary, the Sinterklaas storm and its morphological impact at this site, and the review of relevant previous studies. The description of the XBeach model is given in chapter 3, focused on its key physical processes. Chapter 4 deals with the alternatives generally used to reduce XBeach's often large runtimes—the morphological accelerator factor, or $morfac$, being a mainstream option. Additionally, a model setup is proposed to simulate the Sinterklaas storm at Het Zwin in a workable simulation time, without compromising its accuracy and reliability.

The results of the hind-cast and the required calibration of the model to reproduce the overwash regime are presented in chapter 5. The best set of parameters is later used to analyse a number of hypothetical scenarios in chapter 6.

Finally, chapter 7 discusses the calibration methodology and the unavoidable trade-offs the numerical modeller must face in order to produce reliable estimates in a reasonable time. The main conclusions of this work and suggestions for further research are drawn in chapter 8.

2

Background

2.1. Description of the Zwin estuary

2.1.1. History

Het Zwin is a small natural reserve located at the coastal border between The Netherlands and Belgium. It consists mainly in wetlands of high environmental value connected to the sea trough a meandering tidal channel[1]. An aerial view of Het Zwin is shown in figure 2.1a.

Het Zwin originally was a large estuary in Southern Holland that connected the medieval Belgian town of Brugge with a larger fluvial network and the North Sea. It is believed to have been created after the big storm of 1134 breached the Flemish coastline. Over the past centuries the estuary underwent a strong siltation process which eventually prohibited the transit of vessels. In more recent times the extent of the tidal influence was limited by the construction of dikes around the mouth of Het Zwin[2].

Currently, this "slufter" (as called in Dutch) has an extension of 2.5 km along the coast and 1.5 km inland from the dune line. In all rigour it probably cannot be classified as an estuary given its small extension. Probably the term tidal inlet is better suited, although no back bay or lagoon is present. It is clear, nonetheless, that the system is tide-dominated and all three terms will be used interchangeably in this report.

2.1.2. Morphological development

The Zwin inlet system is morphologically very active; the interaction between the waves, flows and sediments create complex bar patterns in the nearshore zone which are in continuous evolution. The characteristic physical components of the inlet system are the runoff or tidal channel, the flat marshes, and the dunes.

The tide moves salt water in and out of the marshland. At this location the net longshore sediment transport is towars North-East, and this pushes the channel to migrate in that direction. The channel is regularly dredged back into position, in order to keep it aligned with border between Belgium and The Netherlands, and also to avoid damage to the Dutch dunes. In a way, the system is being constrained to avoid its natural development, similar to what is done at the Slufter, at the island of Texel.

Figure 2.2 shows two satellite images of Het Zwin during low tide (2.2a) and high tide (2.2b). The mean tidal range is in the order of 3 to 4 meters in this location, and water enters the slufter mostly through the main channel, which is essentially normal to the shore. Within this channel a series of sand banks and gullies is present, which give a meandering character to the outflow. On the other hand, the inflow occurs over both the gullies and the shoals. Occasionally, very high tides occur which drive water to the farthest parts of the diked area, flowing through both the channels and over the

[1] http://cadzand.org/en/zwin.php
[2] http://www.damme-online.com/gb/nature/zwin.htm

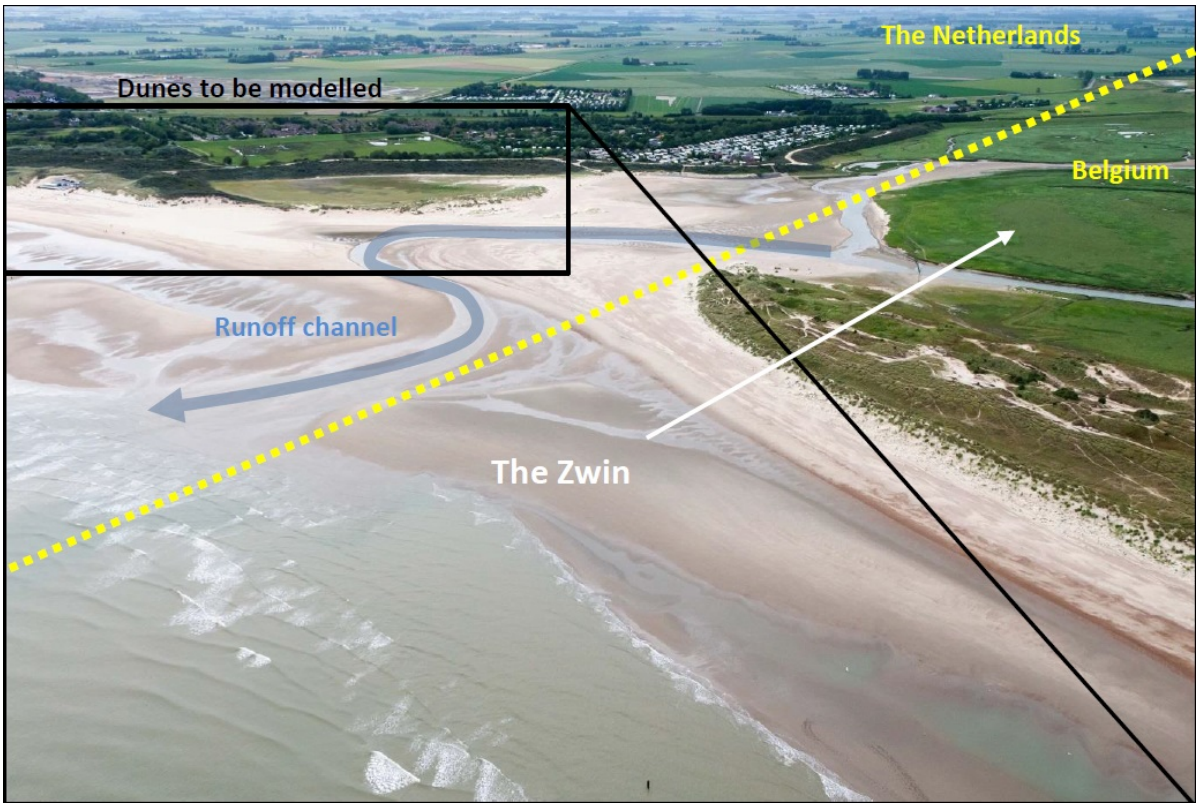

(a) Aerial picture of Het Zwin, The Netherlands. The runoff channel shows a meandring nature, and a set of bars at its mouth. Source: Rijkswaterstaat Image Archive (https://beeldbank.rws.nl/Photos/2967/445068.jpg)

(b) Zoom on the area of interest. The Dutch dunes at the mouth have been curved landward over time. A gap is clearly visible at the mouth, where the dunes present a much lower hight and width.

Figure 2.1: General view of Het Zwin. The coastline is roughly facing NW, The Netherlands being at NE (upper left of the picture) and Belgium at SW (lower right).

(a) Low tide 2005. Source: Google Earth.

(b) High tide 2007. Source: Google Earth.

Figure 2.2: Intertidal areas of Het Zwin. Complex patterns of bars at the mouth and gullies along the channel are observed at low tide. High tide floods large areas, reaching near the dunes.

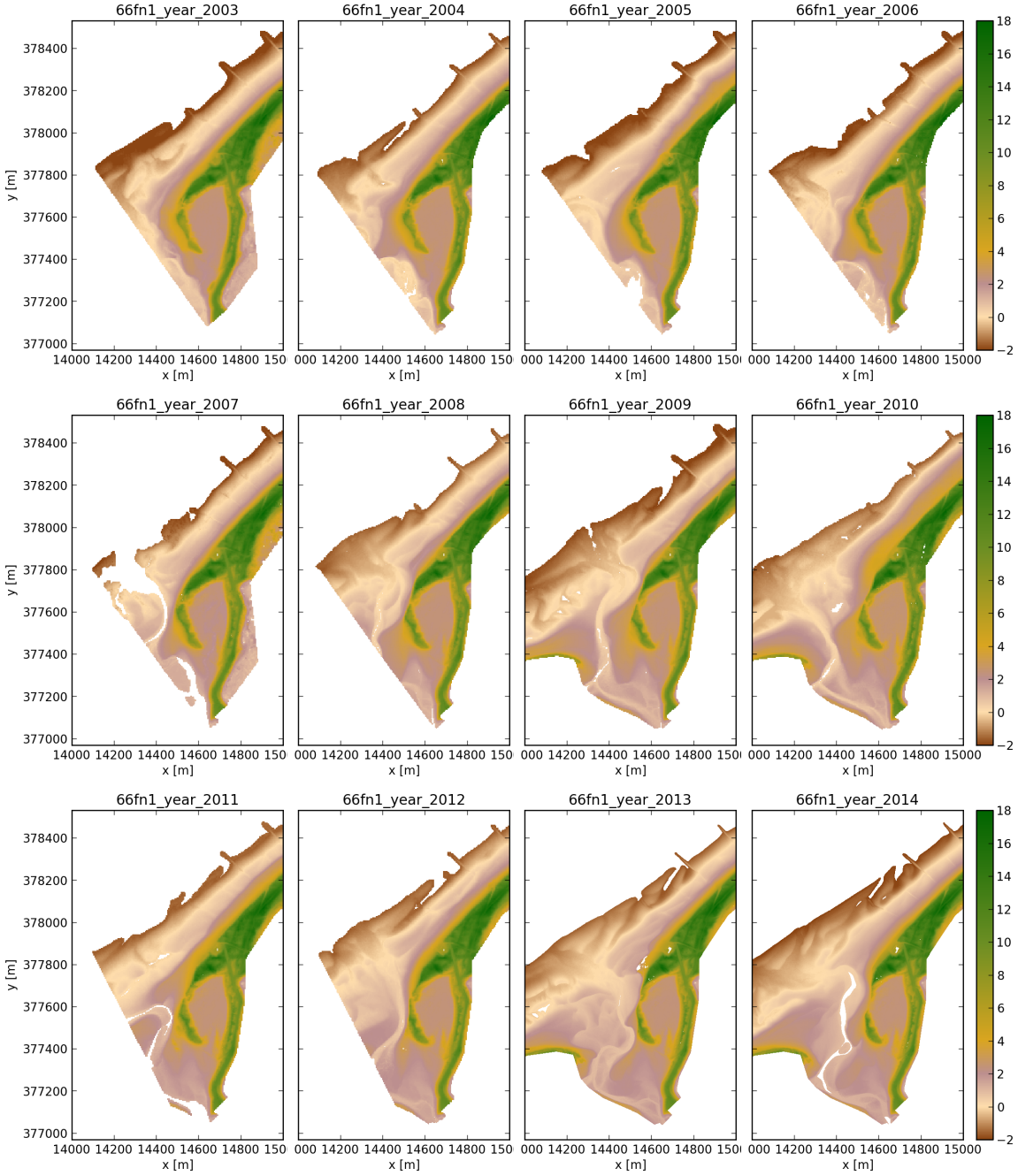

Figure 2.3: Morphological evolution of Het Zwin's dunes. A lower and less wide section has been forming in the Dutch dunes over the years, presumably due to the shifting of the tidal channel position. Scale bar in meters with respect to NAP.

tidal flats. This behaviour has created a reservoir of brackish waters away from the mouth, and makes this small estuary prone to capture sediments, which is evidenced by the higher terrain elevation of Het Zwin as compared with the land beyond the dikes.

Figure 2.2b also shows that during high tide the water almost reaches the toe of the dunes. Hence, during energetic sea states or during higher-than-usual tides (or both) the dunes are susceptible to erosion. Where this eroded sand is normally deposited lies beyond the scope of this thesis, but some options indicate that it can be lost in the lower shoreface, or reworked in the many sand bars of the mouth of Het Zwin, or be transported landward and be deposited over the tidal flats. Most likely the storm will make the sediment suddenly available, and over large time scales it will be redistributed.

Finally, the morphological evolution of the Dutch side of Het Zwin, as recorded by LIDAR altimeters, is presented in figure 2.3. Unfortunately, only during years 2009, 2010, 2013, and 2014 the full coast—i.e. both Belgian and Dutch areas—was measured. Nonetheless, it is possible to observe the translation of the main runoff channel meandering towards the right of the plots. The intertidal area is roughly located between NAP-2 and NAP+2 m.

It would appear that most of the impact on the dunes is done by the tidal channel "lashing" them, as can be seen in years 2008, 2012 and 2013. The frame corresponding to year 2014 shows the effects of the Sinterklaas storm which will be addressed in section 2.3. However it can be stated that the storm partly smoothed out the intertidal area rather than reshaped the dunes. Additionally, it is known that several dredging campaigns were performed during this time span, although the exact execution dates and activities couldn't be verified for this work. It is evident, for instance, that the runoff channel was dredged back towards the Belgian side at some point during 2009, but from the records is hardly possible to say more than that.

From the observations, it appears that the position and shape of the dunes is mostly controlled by long-term processes, in which the position of the main tidal channel seems to be of major importance, whereas stormy event will erode sediment from the upper part of the dunes and make it available for transport. The analysis of the long-term morphological behaviour is beyond the scope of this thesis, which will focus only in the short-term response of the system—and particularly on the overwash phenomenon. It is, however, an interesting topic for further research.

2.1.3. Present-day dunes

The Dutch part of Het Zwin's mouth contains a ~400 m long row of dunes, of varying width (20 to 60 m). The dune heights range between 4 and 15 [m NAP], and present a gap in the center where the row is narrower and lower, as can be seen in figure 2.1b. The top of the dunes shows abundance of vegetation with long roots. Behind the dunes there is a dike that directly protects a camping site and the land farther behind, which is part of the city of Cadzand.

2.2. Storm impact regimes

Sallenger (2000) proposed to classify the morphological impact of storms on barrier islands on four distinct regimes. This classification has been widely spread and currently is also used to asses the impact on beach dunes. The regimes are differentiated depending on the relative positions of the lowest and highest storm-induced water levels, $R_{low} = tide + surge + setup$, $R_{high} = tide + surge + R_{2\%}$, with respect to the dune toe and crest, D_{toe} and D_{high}, respectively.

The regimes are defined as follows

Swash. The wave oscillations remain below the dune toe. $R_{high} < D_{low}$.

Collision. Short waves impact the dune face constantly. $D_{low} < R_{high} < D_{high}$.

Overwash. Short waves runup and overtop the dune crest. $D_{high} < R_{high}$.

Inundation. The whole surge flows over the dune crest. $D_{high} < R_{low}$.

A schematic representation of the four regimes is presented in figure 2.4.

These definitions will be used to characterize the storm impact of the Sinterklaas storm in section 2.3 and to provide background for the scope of similar storms covered in previous studies, presented in section 2.4.

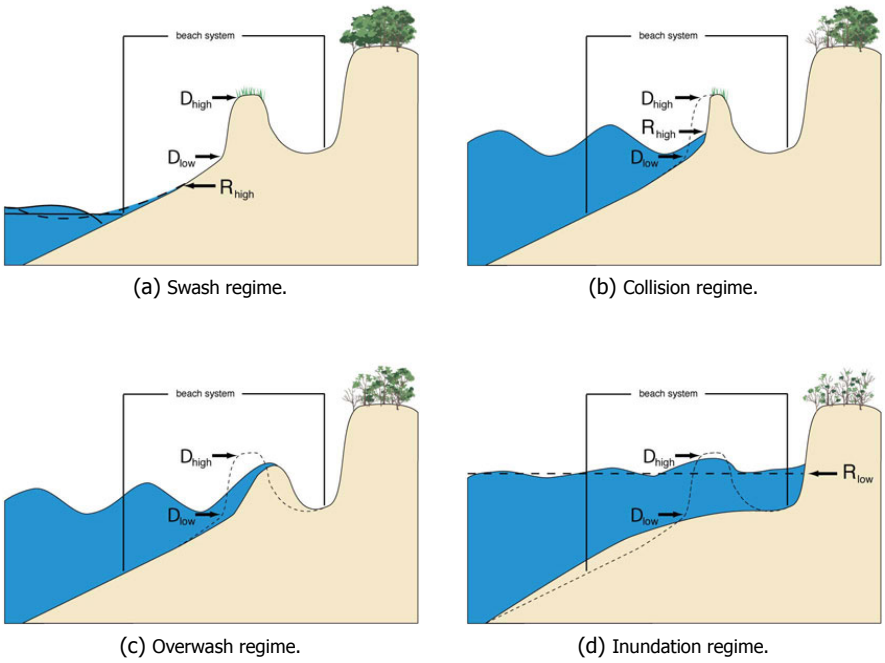

(a) Swash regime. (b) Collision regime.

(c) Overwash regime. (d) Inundation regime.

Figure 2.4: Storm impact regimes as defined by Sallenger. Source: USGS http://coastal.er.usgs.gov/hurricanes/impact-scale/.

2.3. Sinterklaas storm

2.3.1. General description

During the evening of the 5th of December 2013 a severe winter storm hit north-west Europe. The date corresponds with the celebration of the traditional holiday of Sinterlkaas in Dutch speaking countries, hence the adopted name: "Sinterklaas storm". However, the storm is only known by this name in The Netherlands and Belgium. In other countries, particularly in Germany where their effects were more severe, the storm is often referred to as "Cyclone Xavier". The full storm lasted for a few days, until in the final hours of the 7th of December.

The storm was caused by a low-pressure center in the atmosphere travelling from Greenland towards southern Scandinavia which drove high speed winds along its path, mainly over eastern Britain and the south-eastern North Sea coastline. Figure 2.5 shows two maps depicting the forecast path of the storm and its associated wind speeds (2.5a), along with qualitative indications of the actual damage after the first day of the storm (2.5b).

The high winds, with a NE predominant direction, induced high surges and waves throughout the North Sea. A description of the passing front was elaborated by the Dutch Meteorological Institute (Koninkijk Nederlands Meteorologisch Instituut, 2013), which was used to set a red-code warning in the north of the country, where winds were expected to overpass 35 m/s (hurricane force in the Beaufort scale). An animation of the pressure and wind patterns can be retrieved at their website[3].

The Sinterklaas storm caused large material damage, mainly by flooding cities and impacting sandy coasts, causing damage and over 15 casualties in Europe. The impact in The Netherlands was somewhat less severe, although the observed water levels were the highest recorded since the historical

[3] http://www.knmi.nl/klimatologie/daggegevens/weerkaarten/index.cgi

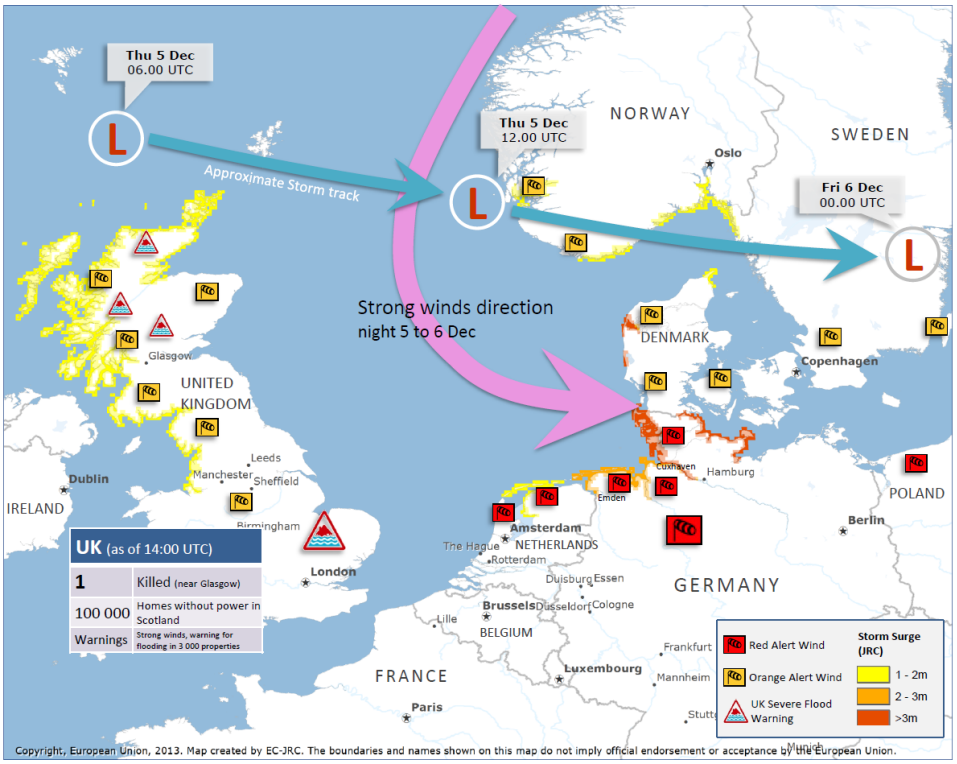

(a) Forecast of the path of the storm (blue arrows) issued the 5th of December. High wind and storm surge alerts were issued for England, Germany, Denmark and The Netherlands.

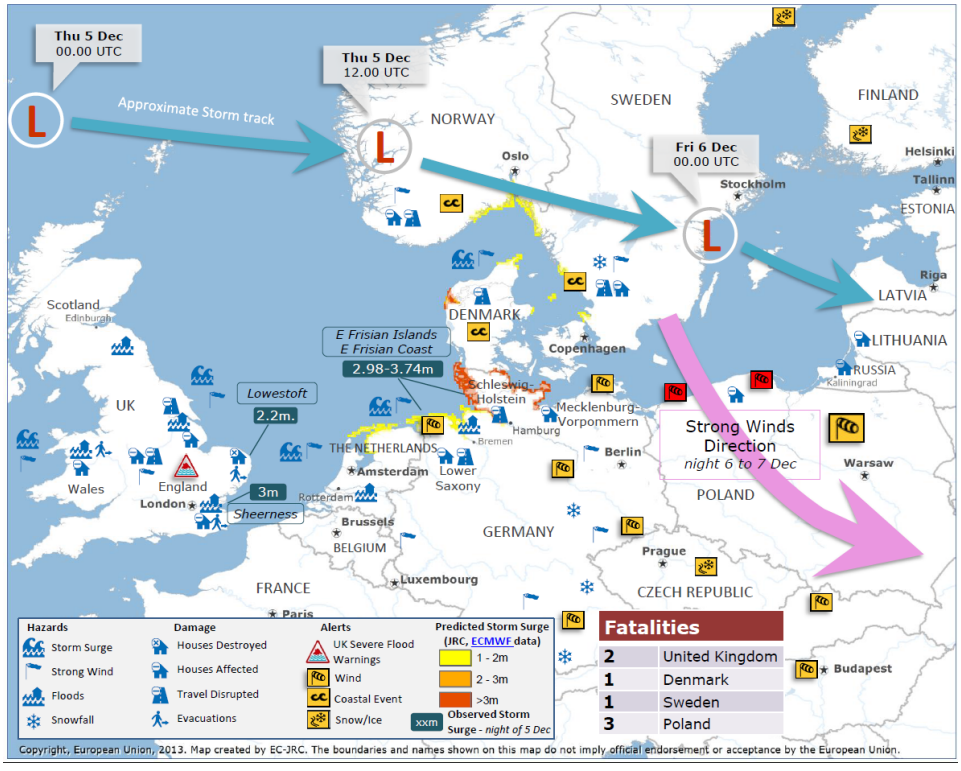

(b) On the 6th of December a preliminary assesment was issued stating the estimated storm surge levels, floods locatoin and type of damage experienced.

Figure 2.5: European Commission forecast (upper panel) and first assessment (lower panel) of the Sinterklaas storm. Source: http://erccportal.jrc.ec.europa.eu/Maps

flood of 1953. In preparation for the peak of the surge all gates of the Easter Scheldt barrier were closed during high tide. Despite minor flooding being observed around Rotterdam, most of the impact of the storm was concentrated along the sandy dunes of the coast.

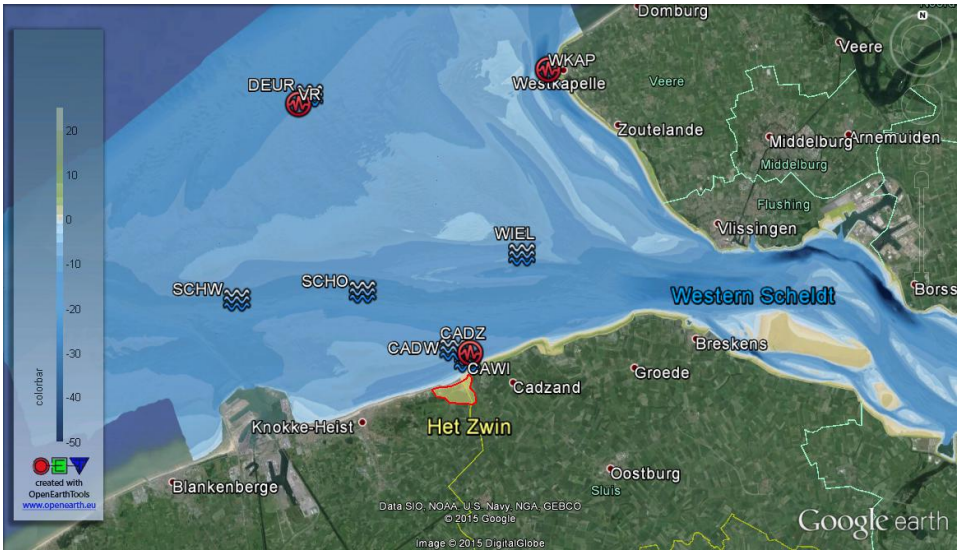

Figure 2.6: Wave buoys (blue wave icons) and tide gauges (red signal icons) locations near the project site. Het Zwin is indicated by a red line. The tidal channel of the Western Scheldt estuary is clearly visible.

The passing of the storm in The Netherlands was recorded by a large network of sensors deployed along the Dutch coast by Rijkswaterstaat (RWS). Figure 2.6 shows the approximate location of wave buoys and water level gauges around the area of interest, i.e. in the south-west end of the province of Zeeland, near the mouth of the Western Scheldt. The system has been recording data dating back several years[4], and the measurements are freely available for download[5] to be used for non-commercial purposes.

Additionally to the oceanographic data measurements, RWS performs periodic measurement campaigns for the height of the dunes along the Dutch coast. The dunes being the first—and in many locations, the only—defence of the hinterland against flooding from the sea, the assessment of their status and maintenance is of key importance. Data is usually collected via airborne *lidar* instruments once per year (dating back almost 20 years), which allows not only to assess the current status of Dutch dunes and beaches, but also their morphological development. This dataset is used in subsection 2.3.4 to estimate the morphological impact of the Stinterklaas storm in the area around Het Zwin.

In the following a description and analysis of the measured wave parameters and water levels will be given, and based on the topographic measurements an estimation of the morphological impact of the storm is made.

2.3.2. Oceanographic conditions

Winds

Figure 2.7 shows the wind records at two locations near Het Zwin: at the city of Cadzand (point `CAWI` in figure 2.6), and 18 km offshore, at the point identified as `VR` (Vlakte van de Raan). The time series indicates the 10-minutes average wind speed at a height of 10 m above the surface, and the wind direction is shown using the nautical convention.

In the plot a steady rise of the wind speed is observed during the first 12 hours of the 5th of December, growing from ~7 m/s to a peak of over 20 m/s in the firs hours of the afternoon, staying above 15 m/s until noon of the 6th, and only returning to pre-storm values during the 7th of December. Following

[4]Usually more that 20 years, depending on the device and location.

[5]`http://waterberichtgeving.rws.nl/nl/water-en-weer_dataleveringen_ophalen-opgetreden-data.htm`

the rising in speed during the 5th, the direction of the wind shifted from 290°N to 240°N, and then varied rapidly to a value that averaged 310°N during the most intense part of the storm. In the first hours of the 7th the direction brusquely changed again to values well below 270°N for a few hours. This behaviour is coherent with the path of the low-pressure center and a clock-wise pattern of winds around it. In general, the velocities at both locations are comparable, although tend to disagree when a difference in the wind direction is present, which is most likely explainable by orographic effects near the station of Cadzand. However, during the most intense part of the storm (from late 5th to early 7th) the agreement between both points is very high.

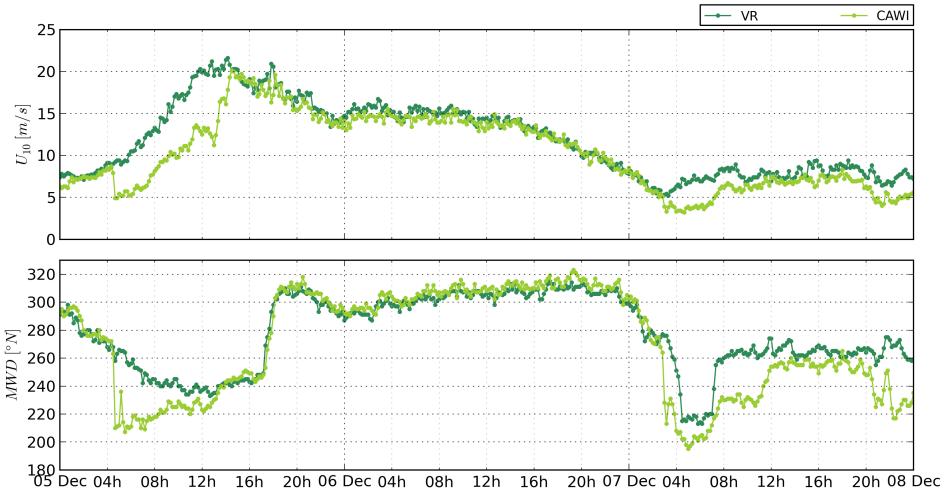

Figure 2.7: Wind conditions measured during the Sinterklaas storm.

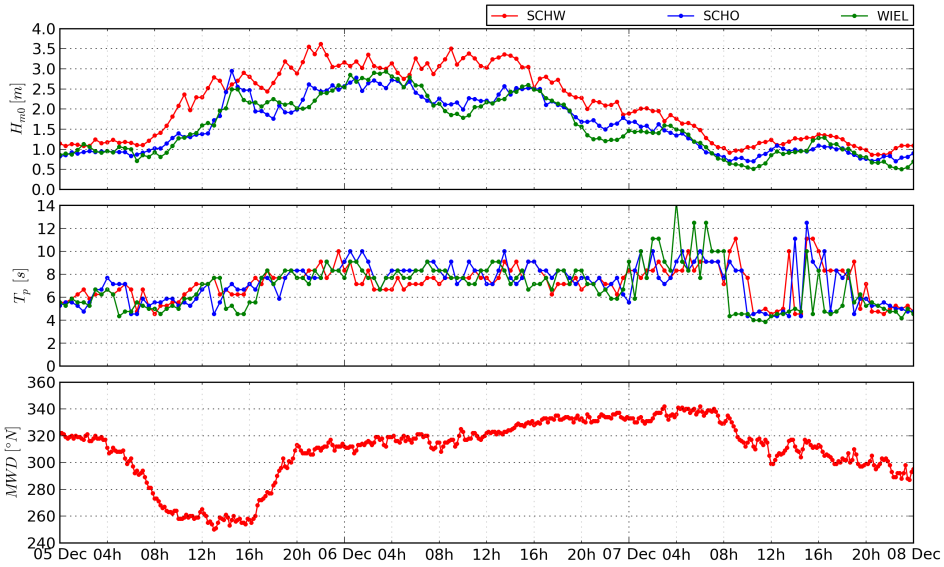

Figure 2.8: Wave parameters measured during the Sinterklaas storm.

Waves

The stormy winds generated seas that propagated all along the North Sea. Particularly at Het Zwin the growth of the waves was limited by fetch—Great Britain is located ~150 km NW of Zeeland, and winds presented a predominantly NW direction—, which made the impact of the storm less severe in the South than it was in the North of The Netherlands, or Germany for that matter.

Figure 2.8 shows the record of wave's parameters during the storm at three locations along the Eastern Scheldt tidal channel closer to the coast: SCHW, SCHO, and WIEL. These locations were selected since

they are suitable to be used as model inputs, as will be addressed in section 5.2. The behaviour of the wave height H_{m0} is similar to the one observed for the wind, this is, increasing during the afternoon of the 5th, reaching a peak in the first hours of the 6th, and then slowly decaying to pre-storm values during the 7th of December. The peak period T_P also experiences an increase, although a more gradual one, changing from 6 s to around 10 s, with values around 8 s during the most severe part of the storm. The direction of the waves, as measured at point SCHW, closely follows the pattern of the wind direction as it would be expected, with directions from around 250°N during the first hours of the 5th rapidly changing to around 320°N in the evening. From that moment until the end of the storm the wave direction slowly changed from somewhere around 310°N to nearly 340°N.

This record is consistent with the lower waves heights registered during the early hours of the storm, despite the fact that during those hours the wind speed were higher; waves from the west not only have a more limited fetch but are also subjected to more refraction, and thus, experience more wave dissipation.

Despite all three points showing a similar pattern, some differences are clear between them. Notably, the point SCHW seems to be more exposed to wave attack than the other two points. This can be explained by the large sand shoal located just to the north of the points SCHO and WIEL which would dissipate part of the incoming energy to those locations. In another words, the point SCHW is located closer to the exit of the tidal channel and therefore is most exposed waves coming from the North Sea.

Finally, the shore normal at Het Zwin is roughly oriented towards 340°N, and therefore the storm largely hit the coast under an angle, especially during the first hours when large wave heights were recorded. It is reasonable to expect the development of intense wave-induced alongshore currents, depending on the refraction patterns of the wave fields during the storm.

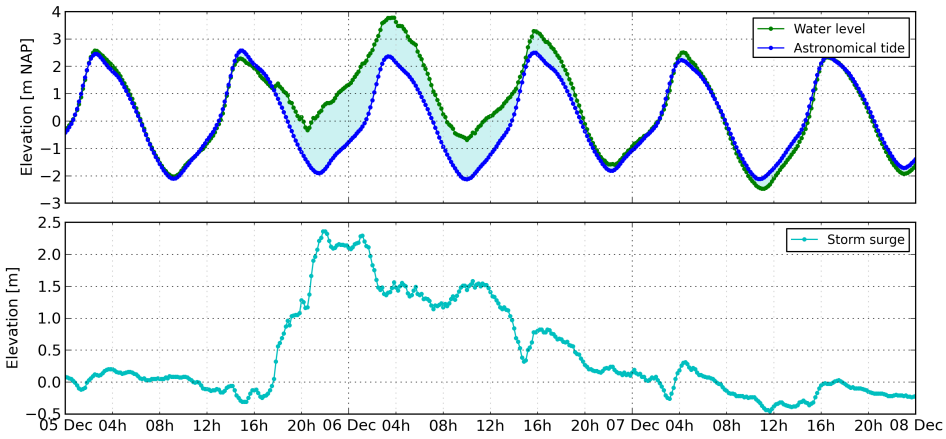

Figure 2.9: Water level and storm surge measured during the Sinterklaas storm.

Water levels

The upper panel of figure 2.9 shows both the forecast astronomical tide and the actual water level recorded during the storm. The difference between them corresponds to the storm-induced surge, which is plotted in the lower panel. The surge starts in the evening of the 5th and in just a few hours it raises to a maximum level of about 2.5 m. Fortunately, this maximum in surge occurred mainly during the rising tide, and hence the actual water surface remained at a reasonable level. During the two following high tides the storm surge had already diminished to 1.5 m and 0.8 m, respectively. The effect of the storm on the water level can be considered to be negligible during the morning of the 8th.

2.3.3. Post-storm site visit

A few days after the storm, Deltares carried out a site visit to Het Zwin in order to determine the impact of the storm on the Dutch dunes. The visit was coordinated with the Scheldestromen Water Board[6]

[6] http://www.scheldestromen.nl/

(which is responsible for maintaining the safety of the coast amongst other things). Figure 2.10a shows a picture taken from Cadzand towards the dune rows, in which the gap in this field is clearly visible.

During the storm the water rose over the foot of the dune and partly submerged it, which is evidenced by the scarping experienced on the dune's front. In short; once a part of the dune is under water, the sand grains become more prone to be moved under the action of flows and waves, which in turn might lead to the collapse of the upper part of the dune that rests on them[7]. Examples of the scarped dunes are presented in figures 2.10b and 2.10c, which correspond to the west and north-west faces of the final dune. The scarping height easily exceeded 2 m at many locations, especially those facing the sea. Large lumps of sand are visible below the toe of the dunes and the failure of the dune's face is observed by the generation of nearly vertical walls in the sand. In this particular case the long roots of the vegetation seem to have helped retaining the sand from falling down, giving a somewhat higher strength to the soil.

This type of impact falls into the "collision regime" described by Sallenger (2000), in which the water level remains above the toe but below the crest of the dune. It was observed that the largest impact occurred in the dunes facing the sea, and particularly near the gap in the dune field, and a somewhat lesser impact occurred near the end of the dune row, towards the inside part of Het Zwin. This difference is probably explained by a larger piling up of water and more sediment availability in the outermost part of the dunes. Additionally, part of the surge is thought to have flown through the gap in the dune row, which might have led to larger flow velocities, enhancing the sediment erosion of the dunes' toes. This flow corresponds to the "overwash regime" (Sallenger, 2000), in which the water level occasionally overpasses the dune crest, flowing over it and normally causing erosion of the top of the dune and deposition on its back.

This was observed in situ and some pictures are presented in figure 2.11. The top panel (2.11a) shows a lateral picture of the gap in the dunes, where the overwash took place. Although not evident, the lighter color of the sand on the right of the image indicates the deposits which occurred during the storm. If inspected closely it is possible to observe that the vegetation along the gap is not straight up, but rather on the ground and curved to the right, as it was swept by the water flowing in that direction. Some debris are also observable in the picture. Moreover, in the back the growing dune field is observed, where the the severe scarping of its front is evident. It is reasonable to assume that part of the sand eroded from the dunes was later transported above the smaller dunes, through the gap, and deposited at the back of the dunes, once the flow velocities decreased. This is observed in the lower panel (2.11b) where the sediments tend to deposit in the fan-shaped fashion, spreading out from the original gap. The extension of this washover fan is relatively small, remaining in the vicinity of the gap.

2.3.4. Estimated impact

The storm impact as inferred from the measurements is only an estimate of the actual impact of the Sinterklaas storm. The main assumption made is that the pre-storm data is representative of the conditions just before the storm occurred, which is debatable. It certainly is a good estimate, but probably improvements are still possible.

Available data

The topography at Het Zwin is regularly measured by RWS to assess the safety against floods from the sea provided the the dunes. These correspond to yearly measurements performed with airborne lidar instruments. The data is gathered, processed and made freely available[8] to be used by the general public. The data can be downloaded as a cloud-of-points of the actual measurements or as numerical grids with a certain desired resolution. The datasets from RWS relevant for the assessment of the Sinterklaas storm are presented in Table 2.1, the pre-storm measurement being carried out in March 2013, and the post-storm one in February 2014.

[7] In principle, the static stability criterion remains the same whether the grains are above or under water, since it is expressed in terms of the submerged weight of the grains. However, the geotechnical failure of an embankment due to toe removal might lead to the impression (or practical criterion) that submerged critical slopes must be smaller than dry ones.

[8] http://nationaalgeoregister.nl

(a) General view.

(b) Scarped dunes facing the channel.

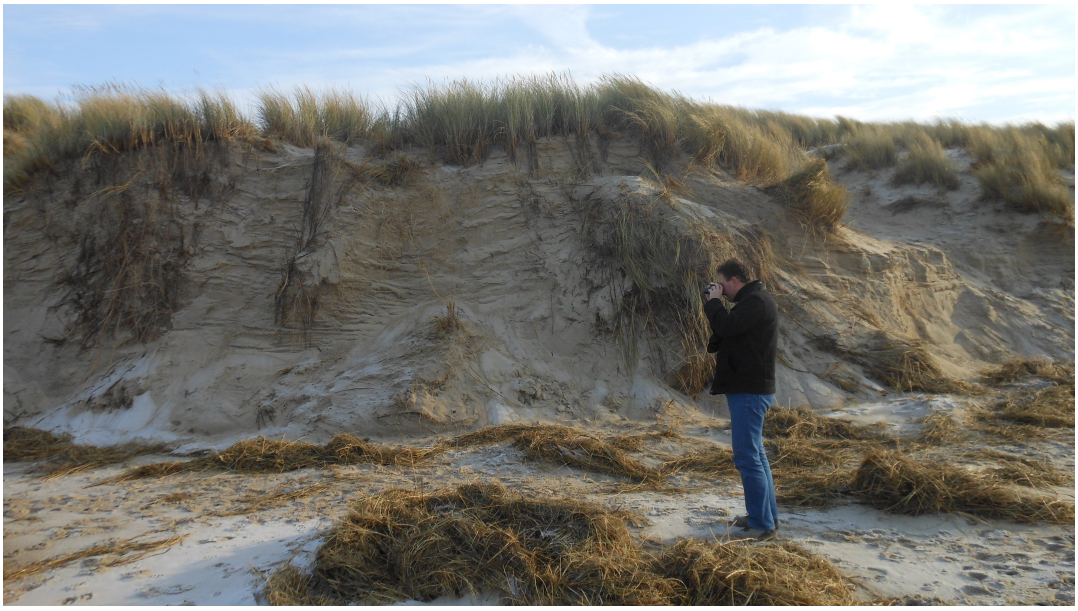

(c) Scarped dunes' front.

Figure 2.10: General view of the Dutch dunes at Het Zwin and records of large portion of the dunes scarped due to the Sinterklaas storm. Photos by Marine Boers, 2013.

(a) Overwash and washed out vegetation.

(b) Washover fan.

Figure 2.11: Record of the overwash event. Photos by Marine Boers, 2013.

Table 2.1: LIDAR campaigns relevant for the storm.

	Date	**Responsible**	Δz [cm]	σz [cm]
Pre-storm	05 March 2013	Rijkswaterstaat	1.6–1.8	1.4–1.5
	29 April 2013	Vlaanderen	1.5	1.8
Post-storm	10 December 2013	Vlaanderen	0.3	2.6
	03 February 2014	Rijkswaterstaat	-	-

However, data processing takes time and it was not completed at the start of this study. Nonetheless, RWS provided direct access to the 2 m resolution gridded data for both pre- and post-storm measurements.

Additionally, data measured by the Vlaanderen government was provided. Moreover, the Flemish decided to carry out an extra measurement flight after the storm in order to capture its impact. The dates of this extra flight and the closest previous one are also presented in table 2.1.

The extension of both datasets is comparable (ranging from the Zeebrugge port in Belgium to the Western Scheldt mouth in the Dutch province of Zeeland) and useful for the purposes of this thesis, as both datasets cover the dunes at Het Zwin at each side of the tidal channel.

Regarding the accuracy of the measurements, RWS requires the error of 98% of the measurements to be smaller that then mean error plus three standard deviations ($\Delta z + 3\sigma z$). In the reports of the Vlaanderen measurements no quality requisite is explicitly mentioned. The values of mean error and standard deviation are indicated in the reports from RWS (Hansa Luftbild/TopScan, 2013, 2014) and the Vlaanderen government (EUROSENSE, 2013, 2014). They are computed as the difference between the measurements and some reference points, and as the normal variation within the measurements. They are presented in Table 2.1, with exception of the RWS' dataset of February 2014, which was not indicated. Despite these values being missing is expectable that they will be in the same range of the rest of the measurements.

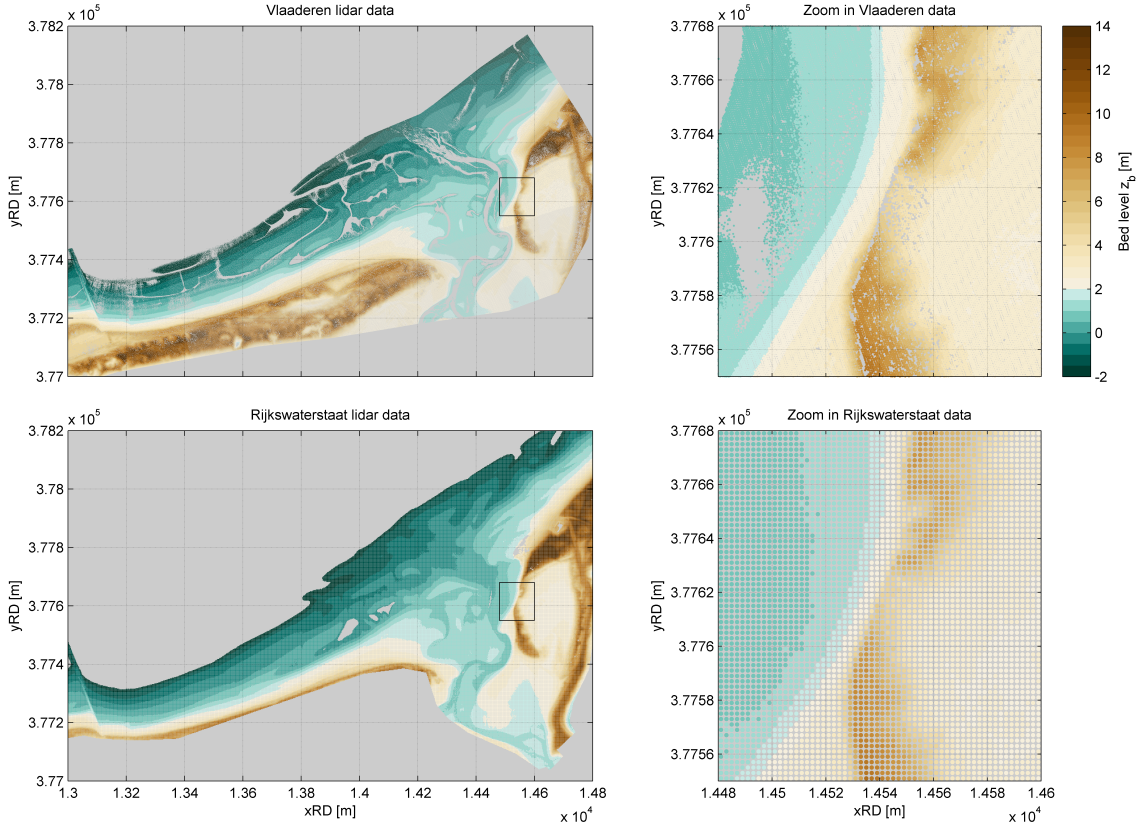

Figure 2.12: LIDAR measurements of the topography prior to the storm. Vlaanderen data from April 2013, RWS data from March 2013.

From this, it can be stated that errors in the data, as compared to the actual terrain height, should be bounded to be far less than 10 [cm] in all datasets. It is outside of the scope of this thesis to perform an analysis of the errors in the measurements, despite the fact that these possible errors, and the way they are smoothed out in the numerical grid, might have a significant impact on the simulation, as pointed out by Plant *et al.* (2002, 2009). The main reason to rule out any further analysis (beside the comparative shortage of time to perform such analysis) is that, for any practical application in

engineering the lidar technology is as good as it gets; detailed in space and accurate in the vertical, relatively fast (per square meter) to measure, and becoming cheaper as technology develops.

Figure 2.12 shows the cloud of points from both datasets around the gap in the dunes. The color of each point indicates its height relative to the NAP level. It is clear from the zoomed plots that the Vlaanderen's datasets cover more densely the gap than the RWS's ones, since the first provided the raw measurements whereas the later provided the data within a grid of 2 m in each direction. The original measurement from both sources included several points in every square meter. Considering that the flow through the gap, i.e. the moving interface between dry and wet cells, might be one of the critical numerical challenges for this project, the Vlaanderen datasets is used as input for the model. Moreover, the time elapsed between the two Belgian campaigns is the shortest possible amongst the sets, with the additional benefit of the post-storm campaign had been carried out just a few days after the storm.

Topographic changes

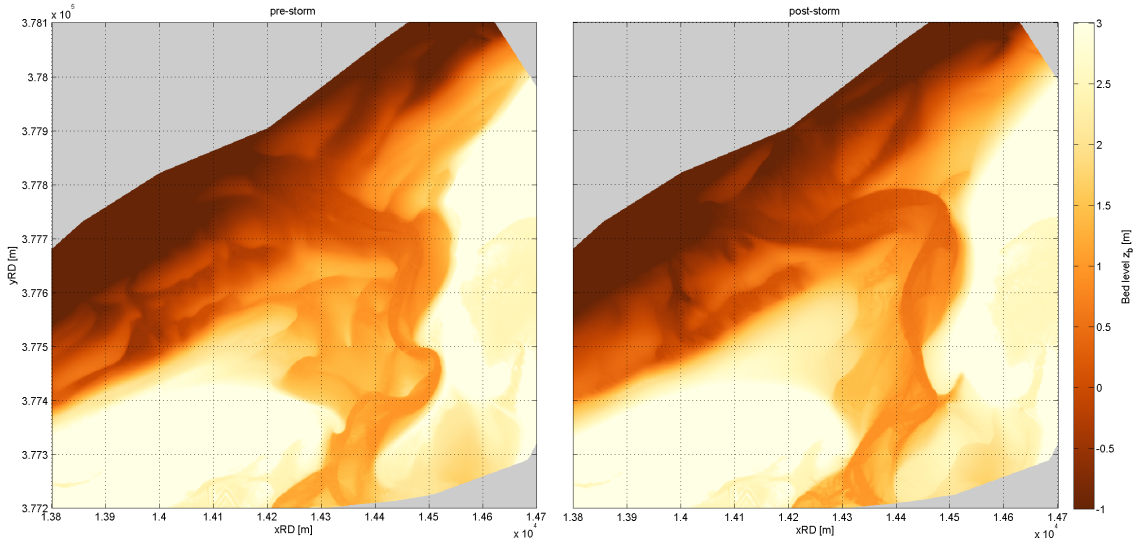

Figure 2.13: Topography of the tidal channel of Het Zwin before and after the Sinterklaas storm.

In order to assess the impact of the storm, the Vlaanderen datasets are considered as representatives of the conditions before and after the storm. They are presented in the left and right panel of figure 2.13, respectively. A qualitative comparison shows at leas two clear effects of the storm: the deepening of the tidal channel, and the overall smoothing of the intertidal topography, which after the storm presents fewer features of smaller wave length.

The difference in topography between both datasets is presented in figure 2.14. The scarping of the dunes is visible at both sides of the tidal channel, at it was particularly intense around the gap in the Dutch dunes, where overwash took place. The deposition fan is also clearly visible at the lee side of these dunes, although its total volume corresponds to only a fraction of the eroded sand from the upper part of the dunes. Apparently, most of the sand was deposited on the tidal channel some 50 meters southward from the gap, shifting the position of the channel farther away from the dunes. This is also evidenced in figure 2.13.

Topographic changes are also observable in the entire upper shoreface, most notably around the tidal channel. These changes are likely to have been caused by the long-term morphological evolution of the system, and hence the influence of the storm on them might be smaller. This is particularly the case for the spit formation at the tip of the Belgian dunes, which tends to intrude into the mouth of the estuary. The volume of sand of the spit cannot be explained solely by the eroded sand from the dunes, and thus its creation is expected to be related with the seasonal longshore transport of sediments along the coast.

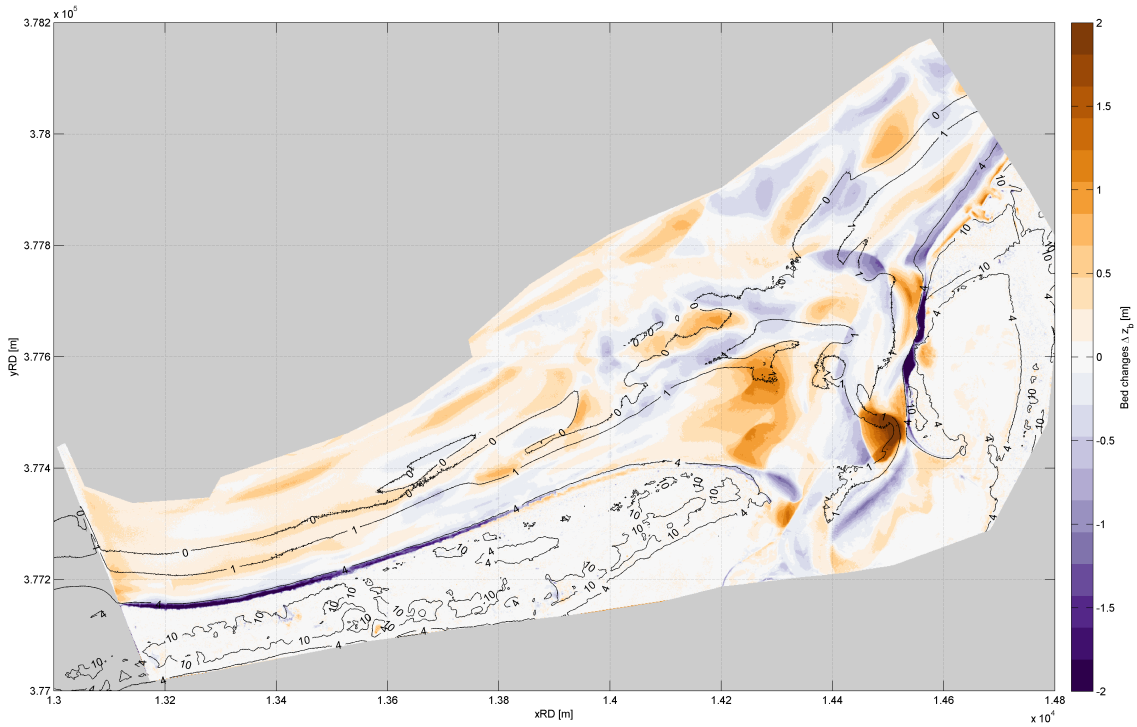

Figure 2.14: Morphological changes as recorded in the lidar datasets.

It must be stressed that the impact of the storm from these datasets can be clearly inferred only for the upper parts of the dunes—which were only been active during this particular storm—whereas the deduction of its impact on the inter-tidal area is less straightforward, as the measurements most likely also include the long-term action of the tide and the longshore currents.

2.4. Relevant previous studies

The impact of the Sinterklaas storm at Het Zwin is studied using the XBeach. This model incorporates most of the relevant physical processes needed to model all four storm impact regimes as defined in section 2.2. For instance, the alongshore variability of the topography has been indicated as a key factor by McCall *et al.* (2010a) and van Santen *et al.* (2012), making XBeach better suited than other more empirical tools—hence, in principle, overwash events should be captured by the model.

However, performing successful hind-casts of overwash regimes bas been a challenging task in the past, and the model has shown a tendency to overestimate the following indicators:

- Erosion volumes.
- Number of breaches in the dune field.
- Extent of the overwash fan.

This might indicate that some of the physics related with overwash are missing in the model. For instance, XBeach doesn't perform any soil mechanics computations, which are indicated by Bisschop *et al.* (2011) to play a critical role in the transport of sediments by high-velocity flows.

McCall *et al.* (2010b) was one of the first in addressing this topic. In order to counterbalance the observed overestimation, they proposed the use of a numerical limiter in the model, namely `smax`, to give an upper limite to the mobility Shield's number. The idea behind this approach is that under high velocity flows dilatancy would increase the soil strength, and thus hinder the pick-up of sediment. In other words, the load on the sediments would only increase up to a certain point. This approach produced satisfactory results and has been widely followed (e.g. Lindemer *et al.*, 2010; Terlouw, 2013;

Stuij, 2014).

The main criticism to the `smax` limiter is that it corresponds to an ad-hoc numerical proxy for underlying processes that are not being actually solved by the model. In fact, de Vet *et al.* (2015) showed that it is possible to limit the amount of erosion during overwash events only by modifying a set of the model parameters, which act together in a similar fashion as the `smax` limiter. He indicated the need of increase both the onshore transport by short-wave asymmetry and skewness, controlled by the parameter `facua`, and the bottom friction of the higher parts of the shoreface. Both processes reduce the erosion volumes by increasing the stability of the dune's toe, and by reducing the flow velocities, respectively.

The calibration was suggested to be taken in two steps: first find the adequate `facua` using a stretch of coast where only collision was observed, and later use that value to find the correct bottom friction to match the overwash patterns. This scheme was followed successfully by Nederhoff *et al.* (2015), who studied the effect of hard structures on barrier islands during overwash events, by hind-casting the impact of hurricane Sandy on New Jersey. They also found that large onshore transport and bottom friction were needed in order to simulate the event, without recurring to the numerical limiter `smax`.

3

XBeach model

3.1. General

XBeach is an event-driven model developed by UNESCO-IHE, Deltares, TU Delft, and the University of Miami, mainly funded by the US Army Corps of Engineers, Rijkswaterstaat and the European Union. The model was originally intended to assess the impact of hurricanes on the barrier islands of the US East coast. However, it is capable to model most morphological changes due to short-term event, such as storms, floods or tsunamis—although most of its applications have been related to dune erosion during storms and hurricanes. The model is developed following an open-source philosophy, in order to improve it in a collective effort and to make it freely accessible. Current and past source codes and executables can be downloaded from the website of the community of developers and users[1].

XBeach is a 2DH shallow water model that fully resolves long waves. Mean flow and the long waves are forced by wind-generated waves, via surf-beating of wave groups and the gradients in the radiation stresses. This requires the model to solve the unsteady short-waves field at the scale of wave groups. Additionally, sediment stirred-up from the bottom and slumped from the dune's face is later transported with the flow depending on the difference between an equilibrium and the computed concentrations. Finally, the bed elevation is updated by conservation of mass of the sediment flows.

The model is solved using a first-order finite differences scheme over a Cartesian coordinate system. Spatial derivatives are computed with an upwind scheme, whereas the non-linear convection terms are schematized in a momentum-conserving form, which allows the model to represent discontinuous water surfaces and to reproduce the flooding and drying processes very accurately. The time-stepping is explicit using the largest possible Δt which ensures stability of the scheme, according to a user defined CFL condition.

In the following, the main characteristics of the hydro and morphodynamics modelled by XBeach are presented. For a detailed description the reader is referred to Roelvink *et al.* (2009, 2010).

3.2. Hydrodynamics

3.2.1. Generalized Lagrangian velocities

The flow in the nearshore is three-dimensional, and the vertical variations are particularly larger inside the surf-zone as short-waves become more non-linear and skewed. The Generalized Lagrangian Mean formulation is an attempt to incorporate this vertical dimension into a 2DH model. This approach states that the difference between the (vertically averaged) Lagrangian velocities—which are experienced by the particles in the flow—and the Eulerian velocities—as observed from a fixed point, say the bottom of the water column—equals the short-wave induced Stoke's drift. Equations 3.1 shows this relation for both components of the velocity u and v, acting in the x and y directions, respectively.

[1] http://oss.deltares.nl/web/xbeach/

$$u^L = u^E + u^S \tag{3.1a}$$
$$v^L = v^E + v^S \tag{3.1b}$$

The Stoke's drift is computed as with equations 3.2, being proportional to the wave-group varying short-wave energy, E_w, oriented in the propagation direction of these wind waves, θ. The other parameters represent the density of water ρ, the total water depth h, and the individual wave celerity c.

$$u^S = \frac{E_w \cos\theta}{\rho h c} \tag{3.2a}$$
$$v^S = \frac{E_w \sin\theta}{\rho h c} \tag{3.2b}$$

This residual flow takes place around mean water level, between the draught and the crest of the short waves, and is (partly) balanced by a return current near the bed: the *undertoe*. It is therefore reasonable to expect the (vertically averaged) Eulerian velocity to be a good estimate of the velocity as "felt" by the bottom, and thus these velocities are used for the interaction with the sediments, whereas the Lagrangian velocities are used to compute the mean and long flow.

In a general form, the short-wave energy equals the integral of the wave spectrum S_w over the frequencies (f) and directions (θ), or equivalently, the wave spectrum represents the distribution of the wave energy density over the range of frequencies and directions. However, XBeach considers all the energy to be concentrated in one representative single frequency bin, $f = f_{m,-1,0}$ as indicated in equation 3.3, in order to minimize the computational effort. This simplification is made on the assumptions of the spectrum being narrow-banded, and that the energy transfer between frequencies is negligible. Additionally, the main objective of solving the distribution of the short-wave energy is to determine the associated infra-gravity waves, which should not be very sensitive to the actual shape of the spectrum (provided it is narrow-banded).

$$E_w = \int\int S_w \,\mathrm{d}f\,\mathrm{d}\theta \quad \xrightarrow{\text{in XBeach}} \quad E_w\big|_{f=f_{m,-1,0}} = \int S_w\big|_{f=f_{m,-1,0}} \mathrm{d}\theta \tag{3.3}$$

3.2.2. Wave-action equations

In order to determine the field of the short-wave energy, it is necessary to solve the so-called wave-action equation (3.4). The wave-action is defined as the energy density over the intrinsic wave frequency (3.5), and corresponds to a conserved quantity that can be transported in the $x - y - \theta$ space with velocities c_x, c_y, and c_θ, respectively.

$$\frac{\partial A}{\partial t} + \frac{\partial c_x A}{\partial x} + \frac{\partial c_y A}{\partial y} + \frac{\partial c_\theta A}{\partial \theta} = \frac{D_w}{\sigma} \tag{3.4}$$

$$A = \frac{S_w}{\sigma(x, y, t, \theta)} \tag{3.5}$$

The propagation velocities in the Cartesian plane are computed as the projection of the group velocity c_g—computed from linear theory—superimposed to the Lagrangian flow velocity, as indicated in equations 3.6. The directional velocity of propagation is computed taking into account both topography and current induced refraction (wave-current interaction), and their interaction with the water depth h and the wave number k. The details of this computation are spared here.

$$c_x = c_g \cos(\theta) + u^L \tag{3.6a}$$
$$c_y = c_g \sin(\theta) + v^L \tag{3.6b}$$

Finally, the right-hand term in equation equation 3.4 represents the wave energy dissipation. The overall dissipation $\overline{D_w}$ is expressed in equation 3.7 as a fraction of the total wave energy, which depends on the relation between the representative (H_{rms}) and the maximum (H_{max}) wave heights expected in that sea state. Further, it is assumed that the mean dissipation is distributed over the directions following the same distribution of the spectrum, which leads to the values of D_w to be used in equation 3.4.

$$\overline{D_w} = \frac{\alpha}{\pi} Q_b \sigma E_w \tag{3.7}$$

3.2.3. Roller energy balance

In an analogous manner, the energy stored in the roller of breaking waves E_r is balanced using its directional spectrum S_r following equation 3.8. In this case, the propagation velocities in the $x-y$ plane are computed based on the wave celerity c instead of the group velocity c_g, whereas the velocity in the θ space is the same as used in the previous subsection. The source term corresponds with the wave-action dissipation D_w, while the sink term D_r is computed to be a fraction of the energy of the roller (3.9).

$$\frac{\partial S_r}{\partial t} + \frac{\partial c_x S_r}{\partial x} + \frac{\partial c_y S_r}{\partial y} + \frac{\partial c_\theta S_r}{\partial \theta} = -D_r + D_w \tag{3.8}$$

$$\overline{D_r} = \frac{2 g \beta_r E_r}{c} \tag{3.9}$$

It is relevant to compute the spectrum of the roller as it contributes to the radiation stresses, and therefore to the forcing of the flow. The total wave forcing is given in equations 3.10 for both Cartesian directions.

$$F_x = -\left[\frac{\partial}{\partial x}\left(S_{xx,w} + S_{xx,r}\right) + \frac{\partial}{\partial y}\left(S_{xy,w} + S_{xy,r}\right)\right] \tag{3.10a}$$

$$F_y = -\left[\frac{\partial}{\partial x}\left(S_{yx,w} + S_{yx,r}\right) + \frac{\partial}{\partial y}\left(S_{yy,w} + S_{yy,r}\right)\right] \tag{3.10b}$$

3.2.4. Infra-gravity waves

Narrow-banded spectra tend to create wave groups that propagate slower than the wave celerity of individual waves. These wave groups produce fluctuations on the short-wave energy and radiation stresses which propagate with the group, and that induce a beating of the "mean water level" which tends to be higher in the zones with lower energy and to be pushed down under high energy, as sketched in figure 3.1.

This phenomenon creates the so-called *infra-gravity* waves (I.G.), which are oscillations in the order of 35 [s], and that are stated to have a major role in the processes of dune erosion by van Gent *et al.* (2008) and van Thiel de Vries (2009). Incoming long waves are *bounded* to the group, since they are forced by it, and hence travel with the group velocity. After breaking, the long waves are released and can interact with the topography at their own celerities, determined by their wavelengths. Xbeach is able to model not only these bound long waves but also the leaky, trapped and edge I.G. (Reniers *et al.*, 2004; van Dongeren *et al.*, 2003) that might appear in the shore once the groups are destroyed by wave breaking.

3.2.5. Long-wave equations

The flow is modelled with the classic shallow-water equations for mass (3.11) and momentum (3.12) conservation, using the Lagrangian velocities aforementioned. The position of the water surface relative to mean water level is denoted by η.

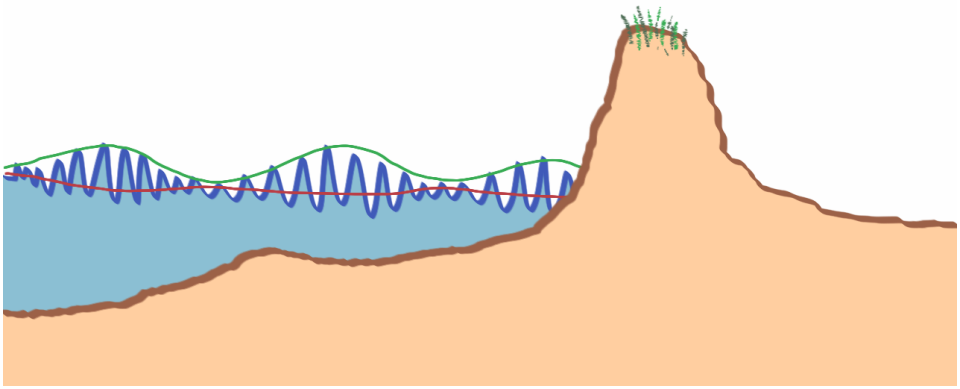

Figure 3.1: Short-wave induced infra-gravity wave. Bound long wave.

$$\frac{\partial \eta}{\partial t} + \frac{\partial h u^L}{\partial x} + \frac{\partial h v^L}{\partial y} = 0 \tag{3.11}$$

The momentum equations include the effects of Coriolis, via its parameter f and horizontal mixing with a turbulent viscosity ν_h. The flow is driven by differential shear stresses between the free surface τ_s (caused by wind) and the bottom τ_b (evaluated using the Eulerian velocities), short-wave forcing F_x and F_y, and gravity (through the gradient in the free surface).

$$\frac{\partial u^L}{\partial t} + u^L \frac{\partial u^L}{\partial x} + v^L \frac{\partial u^L}{\partial y} - f v^L - \nu_h \left(\frac{\partial^2 u^L}{\partial x^2} + \frac{\partial^2 u^L}{\partial y^2} \right) = \frac{\tau_{sx}}{\rho h} - \frac{\tau^E_{bx}}{\rho h} - g \frac{\partial \eta}{\partial x} + \frac{F_x}{\rho h} \tag{3.12a}$$

$$\frac{\partial v^L}{\partial t} + u^L \frac{\partial v^L}{\partial x} + v^L \frac{\partial v^L}{\partial y} + f u^L - \nu_h \left(\frac{\partial^2 v^L}{\partial x^2} + \frac{\partial^2 v^L}{\partial y^2} \right) = \frac{\tau_{sy}}{\rho h} - \frac{\tau^E_{by}}{\rho h} - g \frac{\partial \eta}{\partial x} + \frac{F_y}{\rho h} \tag{3.12b}$$

3.3. Morphodynamics

3.3.1. Transport

The sediment transport is modelled with an convection-diffusion equation, using the Eulerian velocities (3.13). The sediment concentration C represents the vertically averaged concentration, and it includes contributions from both suspended sediment and bed-load. Horizontal mixing is achieved using a sediment diffusion coefficient D_h.

$$\frac{\partial hC}{\partial t} + \frac{\partial hCu^E}{\partial x} + \frac{\partial hCv^E}{\partial y} + \frac{\partial}{\partial x}\left(D_h h \frac{\partial C}{\partial x} \right) + \frac{\partial}{\partial y}\left(D_h h \frac{\partial C}{\partial y} \right) = \frac{hC_{eq} - hC}{T_s} \tag{3.13}$$

Sediment is driven whenever exist a difference between the actual concentration and a certain equilibrium concentration C_{eq}, computed with equation 3.14, in which $|V|$ represents the magnitude of the velocity (considering flow and short-wave contributions), u_{rms} is a representative measure of the short-wave orbital velocity, U_{cr} stands for the critical Shields number (below which no erosion occurs), and A_{sb}, A_{ss} are numerical parameters. This formula corresponds to the current default in XBeach, labelled as the *van Thiel – van Rijn* formula, but other options (with different exponent and constant) are also available to be chosen.

$$C_{eq} = \frac{A_{sb}}{h}\left(\sqrt{|V|^2 + 0.64 u_{rms}^2} - U_{cr} \right)^{1.5} + \frac{A_{ss}}{h}\left(\sqrt{|V|^2 + 0.64 u_{rms}^2} - U_{cr} \right)^{2.4} \tag{3.14}$$

The time scale of transport is determined by T_s, which depends on the particles settling velocity, being larger for finer sediment and smaller (nearly instantaneous) for coarser material.

3.3.2. Wave asymmetry and skewness

Short waves are solved averaged over their phase in XBeach, thus the residual flow induced by them has to be explicitly introduced in the model via an ad-hoc parametrization. These kind of flows, such as the Longuet-Higgins streaming, are caused by non-linear effects characterized by the wave asymmetry (A_s) and skewness (S_k). The magnitude of the flow in XBeach is controlled by the `facua` parameter, as shown in equation 3.15, which is presumably dependent on the grain size of the beach to be modelled (Roelvink *et al.*, 2010). This parameter has a nominal range of $\texttt{facua} = 0.1 - 0.3$, with a default value of 0.1, which is thought to be representative of the coast of Holland (see van Thiel de Vries, 2009).

$$u_A = fac_{u_a} \cdot u_{rms} \left(S_k - A_s\right) \tag{3.15}$$

The overall effect of this short-wave-induced current is to enhance the onshore sediment transport.

3.3.3. Avalanching

During stormy events the higher sections of the shoreface are temporarily exposed to wave attack, and thus prone to be eroded. Normally, the dunes present a steeper slope above the toe, and when they fail under the wave motion big slumps of sand are scarped vertically from these sand walls. Most of the sand made available for transport during storms is eroded from the dunes by avalanching.

This failure mechanism of the soil is represented rather crudely in XBeach, based more on observations of actual beach profiles after storms than in the failure mechanics of the sandy soil. Equation 3.16 represents a maximum critical slope m_{cr} to be forced on the topography of the model: whenever the gradient in bed elevation of two contiguous cells surpasses m_{cr} sediment will be exchanged between them in order to lower the slope. Additionally, the model makes a distinction on this critical slope depending on the flooding status of the numerical cells: wet cells allow a much milder slope, whereas dry cells can present steeper slopes. In this way, the original beach profile can only be modified under the action of the water. In short, the storm surge lowers the maximum allowable slope releasing sediment from the upper part of the dune, which is later transported mainly by infra-gravity motions.

$$\left|\frac{\partial z_b}{\partial x}\right| > m_{cr} \tag{3.16}$$

Crude as it may be, the avalanching representation in XBeach produces dune profiles that compare well with measurements, which would significantly differ should the avalanching would be turned off. Hence, the avalanching algorithm is of key importance in the modelling of storm impact.

3.3.4. Bed updating

Once the sediment is transported by the flow, a mass balance is performed in order to compute the bed level change as shown in equation 3.17, in which q_x and q_y correspond to the mass fluxes on both Cartesian directions, p represents the soil porosity (typically $p \simeq 0.4$), and f_{mor} stands for *morphological acceleration factor* (e.g. Reniers *et al.*, 2004).

This numerical factor is intended to reduce the number of computations to be taken in the model, and thus speed up its runtime. It works in two ways; on one hand it "squeezes" the time series of the hydrodynamic inputs by a certain factor, making them shorter, and on the other hand in amplifies the morphological changes each time step by this same factor. The recommended range of values for this accelerator is $f_{mor} = 1 - 10$. The XBeach parameter controlling the morphological acceleration is `morfac`.

$$\frac{\partial z_b}{\partial t} + \frac{f_{mor}}{(1-p)}\left(\frac{\partial q_x}{\partial x} + \frac{\partial q_y}{\partial y}\right) = 0 \tag{3.17}$$

Finally, the sediment flows are computed taking into account both the convection by the flow (as experienced near the bottom) and the sediment diffusion (or lateral mixing) governed by D_h, as presented

in equations 3.18, and the new elevation of the bottom can be computed, and used as input for the next time step of the model.

$$q_x = hCu^E + D_h h\frac{\partial C}{\partial x} \tag{3.18a}$$

$$q_y = hCv^E + D_h h\frac{\partial C}{\partial y} \tag{3.18b}$$

4

XBeach runtime optimization

"If brute force doesn't work, you're not using enough."

— Unknown

4.1. Introduction

XBeach is a relatively expensive computational model to run. This is due to its process-based nature (many relevant processes are being modelled simultaneously), which leads to an intense use of both the computer's processor and memory. From a practical point of view, a numerical model of an event-driven morphological event should run in a period of a few hours, over-night or at a maximum a couple of days.

Actually, this is a central issue in morphological modelling (and in all fields of computational hydraulics, for that matter) where long-term behaviour of the topography is forced and modelled by shorter-term hydraulic conditions. In a way, numerical modelling is a lot about compromise. First the physical laws that govern the phenomenon have to be determined, later they might have to be reduced (e.g. vertically averaged), then they need to be discretized in order to be solved by a computer, and finally the simulated time and the domain extension have to be such as to allow the computations to be done in a workable time. In this thesis, the focus will be in this last point, which lies in the domain of the modeller rather than in the developer's.

In this chapter the relatively long running times of XBeach models will be discussed. First, the dependency of the runtime on the grid resolution will be estimated. The contradictory requirements of high resolution at a reasonable runtime are a daily challenge for modellers, and a fair compromise is paramount in morphological modelling. Next, the traditional ways in which XBeach has been accelerated are briefly reviewed, and two relatively new approaches are presented and applied to the Sinterklaas storm at Het Zwin case in order to test their validity and performance. Finally, a mix of all the measures is selected to be used in the actual hindcast modelling of the storm.

4.2. Runtime estimation

One could make a crude estimate of the expected runtime of a particular model by estimating the number of time steps to be taken, and the time needed to perform each of these steps. Let's picture a standard XBeach model with dimensions L_x and L_y, to be used to simulate a time T_{end}. Let's assume the numerical grid has a mean spatial discretization Δx, and thus $m = L_x/\Delta x$ and $n = L_y/\Delta x$ nodes in each direction. Further, if the model presents a mean time step Δt, the total number of steps to be taken during the modelling is $n_{steps} = T_{end}/\Delta t$. The total runtime will have the form of equation 4.1 in which the function $F(\bullet)$ represents a measure of the time or resources needed for the model to advance one time step in the computation.

$$runtime = n_{steps} \cdot F(m, n, \dots) \tag{4.1}$$

The algorithm analysis of the XBeach code is far away from the scope of this thesis, however it is possible to make general remarks. There seems to be two main tasks that concentrate much of the computation resources: the wave propagation and the output handling.

Wave propagation. According to the general opinion of developers and specialized users, most of the computation power is used in solving the unsteady, spatially varying wave field. This is largely due to the fact of this process being iterative (in contrast to the long wave computation which is actually explicit in time). Despite the fact that the spectrum is only distributed over the directions (it is assumed to be a narrow spectrum concentrated around one representative frequency $f_{m,-1,0}$), the runtime is still considerable. The `single_dir` option is available to compute the mean wave direction based on Snell's law instead of actually computing the spectrum, however the gain in speed is relative to the specification of the directional grid in both cases.

NetCDF output. As it is currently implemented, XBeach creates one large *netCDF* file with the preallocated space to store the required outputs, and then fills up the variables at the specified times as they are computed. This implies to handle in memory an open file for the whole run, which for large models and long runs might lead this output file to have an unmanageable size. Of course, there are other output options, such as saving each variable in a separate file or using text files, but netCDF is a standard file type in hydraulic modelling, and the default on XBeach.

It is reasonable to assume that the runtime of the wave propagation will be determined by the size of the grid $m \cdot n$ and the output handling will depend on its size $m \cdot n \cdot n_{steps}$, most likely in a non-polynomial way. For the sake of the argument it will be assumed that both follow an exponential behaviour, as shown in equation 4.2, in which α and β represent some exponents to be determined.

$$F(m, n, \dots) = e^{(m \cdot n)^{\alpha}} \cdot e^{(m \cdot n \cdot n_{steps})^{\beta}} \tag{4.2}$$

It is possible to reduce this expression considering the dependency of the variables with Δx. Particularly the time step is computed explicitly following the CFL (4.3) in which the celerity of the wave has been used as a representative velocity.

$$\Delta t \leqslant \frac{CFL\Delta x}{\sqrt{gh}} \tag{4.3}$$

Hence the time needed to take one singe time step has the following form:

$$\begin{aligned} F(m, n, \dots) &= e^{(m \cdot n)^{\alpha}} \cdot e^{(m \cdot n \cdot n_{steps})^{\beta}} \\ F(m, n, \dots) &= e^{\left(\frac{L_x L_y}{\Delta x^2}\right)^{\alpha}} \cdot e^{\left(\frac{L_x L_y}{\Delta x^2} \cdot \frac{T_{end}}{\Delta t}\right)^{\beta}} \\ F(\Delta x) &= e^{\left(\frac{L_x L_y}{\Delta x^2}\right)^{\alpha}} \cdot e^{\left(\frac{L_x L_y T_{end} \sqrt{gh}}{CFL \Delta x^3}\right)^{\beta}} \\ \Rightarrow F(\Delta x) &\propto e^{\frac{1}{\Delta x^3}} \end{aligned} \tag{4.4}$$

Therefore, the total runtime is likely to be also an exponential function of the grid resolution, as shown in equation 4.5. This is particularly problematic when flooding and drying processes are expected to be relevant in the case to be modelled (as it is in the overwash regime), since this requires a sufficiently fine grid to resolve these phenomena. However, it is clear that decreasing the cell size by half will lead to a runtime far larger than 4 times (keeping all other parameters constant, and depending on the actual values of α and β, but the point remains valid).

$$runtime \propto \frac{1}{\Delta x} \cdot e^{\frac{1}{\Delta x^3}} \tag{4.5}$$

4.3. Traditional approaches

Traditionally, XBeach users have tried to minimize its runtime by using one, or many of the following options:

Computer clusters. The idea is pretty simple. Use a network of (normally high-performance) computers to run simultaneously several runs, without "clogging" one's own computer.

Parallel computing. This approach is more elaborate since it requires the model to be coded in such a way that it can make full profit of the computer's multiple cores. Basically, sub-domains of the model are computed in different processors, while information is passed along between them by the model. This actually reduces the runtime of a particular run, as opposed to the previous method. Nonetheless, it is clear that parallel models can be run in a computer cluster (as they normally are), and that this leads to further reduction of the total runtime of a *batch* of runs.

However, the reduction in runtime is bounded. On one hand, commonly one of the sub-domains is constantly the slowest in performing its computations, and thus the rest have to "wait" for it before resuming their own computations. On the other hand, increasing the number of sub-domains (provided there are enough processors to do so) will eventually *slow down* the computations, as much of the time will be used in exchanging data between the sub-domains rather than in actual computations. Experience indicates most reduction of the runtime is achieved using 4–8 nodes. This is done in XBeach using a free message passing interface (MPI).

Morfac The use of the morphological acceleration factor, described in 3.3.4, differs drastically from the previously stated methods. Its intention is to reduce the length of the model to be run rather than to perform that run faster. The direct cost to pay for its use is the "bending" of the hydrodynamics of the model, which might in turn affect or modify the morphodynamic response of the system. A more detailed discussion about the use of the `morfac` option in XBeach is presented in section 7.4.

For the particular case of the Zwin model, it is impossible to use a `morfac` larger than one, and thus only the first two options afore mentioned can be employed. The reason for this is that the water level behind the dunes (normally called the "back-bay" in barrier island terminology) depends on the flow through the runoff channel, and hence a modification of the time scale of the tide will produce non-physical water levels (and velocities) at the mouth of the estuary and behind the dunes. A similar case was reported by van Rooijen and van Thiel de Vries (2014), who modelled the storm impact at the Slufter tidal inlet in the Texel island.

This restriction makes the runtime way too long for using a rectangular grid. In the following two alternative approaches are presented and their performance evaluated in order to determine a more suitable scheme to perform the Sinterklaas storm hindcast.

4.4. Proposed approaches

Two alternatives to the use of rectangular grids are presented: switch to use curvilinear grids, and nesting a finer grid dedicated to morphological computations into a larger, coarser grid used only to determine the hydrodynamic inputs for the first one.

4.4.1. Model setup

In order to test the suitability of each approach, both methods were tested using the peak conditions of the storm, showed in figure 4.1. The water level (tide + surge) as recorded at `CADZ` was assumed to be representative. The buoy of point `SCHO` was used to characterize the wave conditions, except from the mean wave direction which was assumed to be the same as recorded at point `SCHW`, which is the only point with records of direction. This point is located in front of the Zwin mouth, at a deeper location over a tidal trench. Between this trench and the coast lies a shallow shoal that will refract and dissipate the waves in a way hard to determine a priori.

The deeper bathymetry was obtained from the Vaklodingen dataset (Wiegman *et al.*, 2005), the most recent measurements dating back to 2011, whereas the topography of the dunes was obtained from

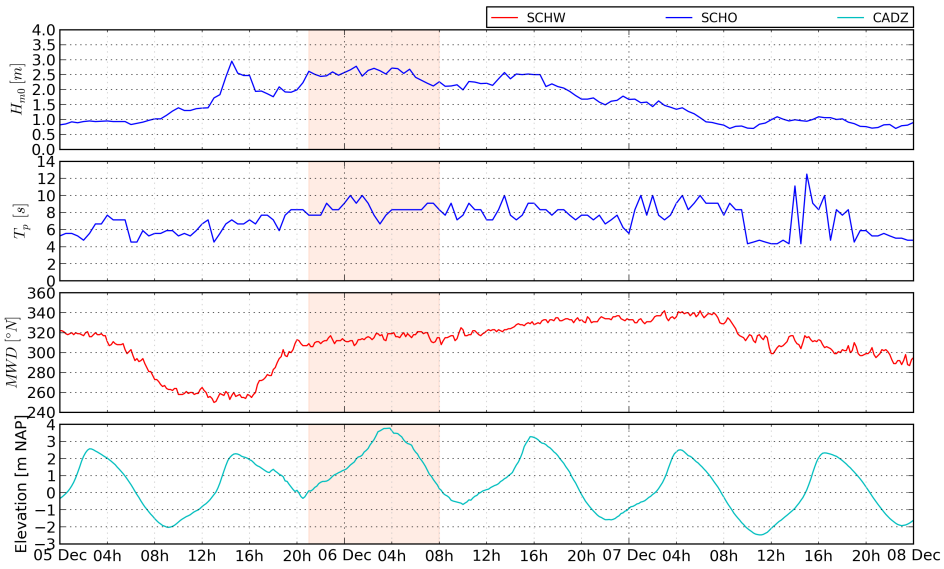

Figure 4.1: Hydrodynamic inputs. Significant wave height, peak wave period, and mean wave direction are presented in the first three top panles. Water level is shown in the lower panel. The color of each line indicates the location of the measurement. Highlighted is the modelled period.

the lidar survey carried out by the Vlaanderen government in April 2013 (EUROSENSE, 2013). All horizontal positions have been expressed in the RD (Rijks-Driehoek) coordinate system, whereas vertical elevations are indicated relative to the NAP (Normaal Amsterdams Peil) datum, which is approximate equal to mean sea level at Het Zwin.

4.4.2. Curvilinear grid

Curvilinear grids present a few advantages over rectangular ones. Particularly for this case, they allow to concentrate higher resolution cells on morphological active areas, and to incorporate a wider range of wave directions which might present large obliquity with the coast. In short, the allow a more precise representation of the hydrodynamic forcing, at the same precision, but using grids with less cells, which allows for shorter runtimes.

The use of curvilinear grids has recently increased among XBeach modellers (e.g. Roelvink *et al.*, 2012, 2013; van Santen *et al.*, 2012) with satisfactory results. Nevertheless, the use of rectangular grids remains a regular practice. The readily available tools[1] to create rectangular XBeach models might explain this trend. Models created this way are easy to be scripted and modified, in contrast with the more "hand-made" construction of the curvilinear grids (a process that might be tedious, less traceable, and more prone to errors by new users). Moreover, smoothness and curvature of curvilinear grids must be bounded to small values in order to create meaningful simulations, the idea behind this is that the grid is reasonably orthogonal in the vicinity of each cell. This might be an extra dissuasion for people wanting to try using curvilinear grids.

A comparison was carried out between the two types of grids. A schematic representation of both grids[2] is given in the first column of figure 4.2. Both grids extend offshore beyond the trench after the shoal, in order to incorporate its refraction effect on the waves, and the wave boundary of the curvilinear grid has been curved in order to incorporate more oblique waves from the NW without producing shadow zones. The bathymetry beyond the trench has been flatten out to a value of -15 [m NAP]—as shown in the second column—which roughly corresponds to the deepest part of the trench.

A comparison has been made between the root mean squared wave height propagation pattern, considering the whole simulation. The results are presented for the entire grid in the third column, and for smaller area near the mouth of Het Zwin, in the fourth column. A very good agreement is found

[1]Via the Open Earth initiative: https://publicwiki.deltares.nl/display/OET/OpenEarth
[2]Each cell drawn in the figure actually represents 5 cells in each direction.

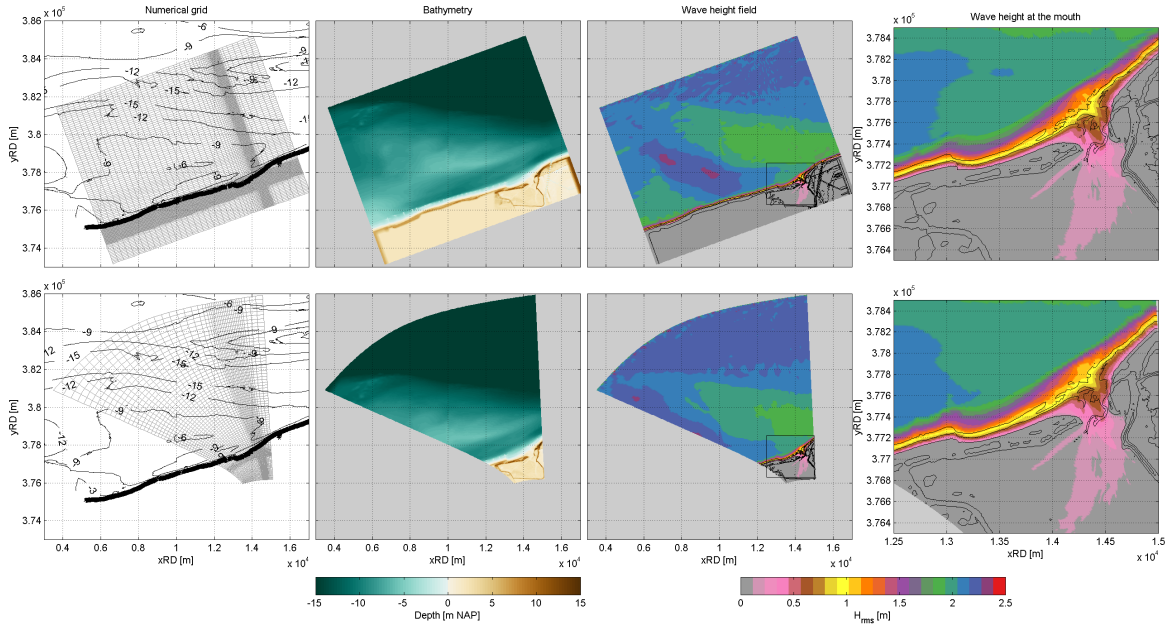

Figure 4.2: Rectangular (upper panels) versus curvilinear (lower panels) grid approach setup. First column schematically show the numerical grids over the measured bathymetry, while the actual bathymetry used in the model is presented in the second column. Third and fourth columns shown the root mean square wave height for the whole domain and a zoomed area near Het Zwin's mouth, respectively.

between them, despite the unavoidable differences caused by the different discretizations and locations of the boundaries, for instance. It is apparent that the modelling of the waves can be achieved successfully with either type of grid.

A more detailed comparison is presented in figure 4.3, where time series obtained using both grids are shown. The points of extractions are indicated in the left panel of the figure, and are located along the tidal channel and before and after the dune gap. The records show a very good agreement in water level, wave height, and flow velocity predictions, the latter showing some occasional phase differences but consistently keeping a comparable amplitude. There are no records of wave height at the lee side of the dunes, and the water levels there during the storm (as observed in the model) actually correspond to water flowing from within the estuary rather than overwashing the dunes.

This can be observed when comparing the morphological impact of the storm as modelled by the two grids, presented in figure 4.4. Both patterns are fairly similar, showing erosion of the dune's fronts and deposition of that material below the toe, at the edge of the runoff channel. Neither presents erosion of the gap nor deposition behind the dunes, indicating that those models did not reproduce the overwash. This is directly linked to the grid resolution in the area of interest, which in both cases was about $\Delta x \approx 5$ m. Hence, the need for a finer grid—and more computational effort—is readily seen.

Finally, table 4.1 presents the size of the grids used in this comparison and their runtimes. It is clear that the use of fewer grid cells leads to a dramatic decrease in time consumption, which in this case is reduced by half.

Table 4.1: Rectangular and curvilinear runtime.

	Rectangular	**Curvilinear**
nx	594	461
ny	336	232
runtime [hr]	42.4	19.9

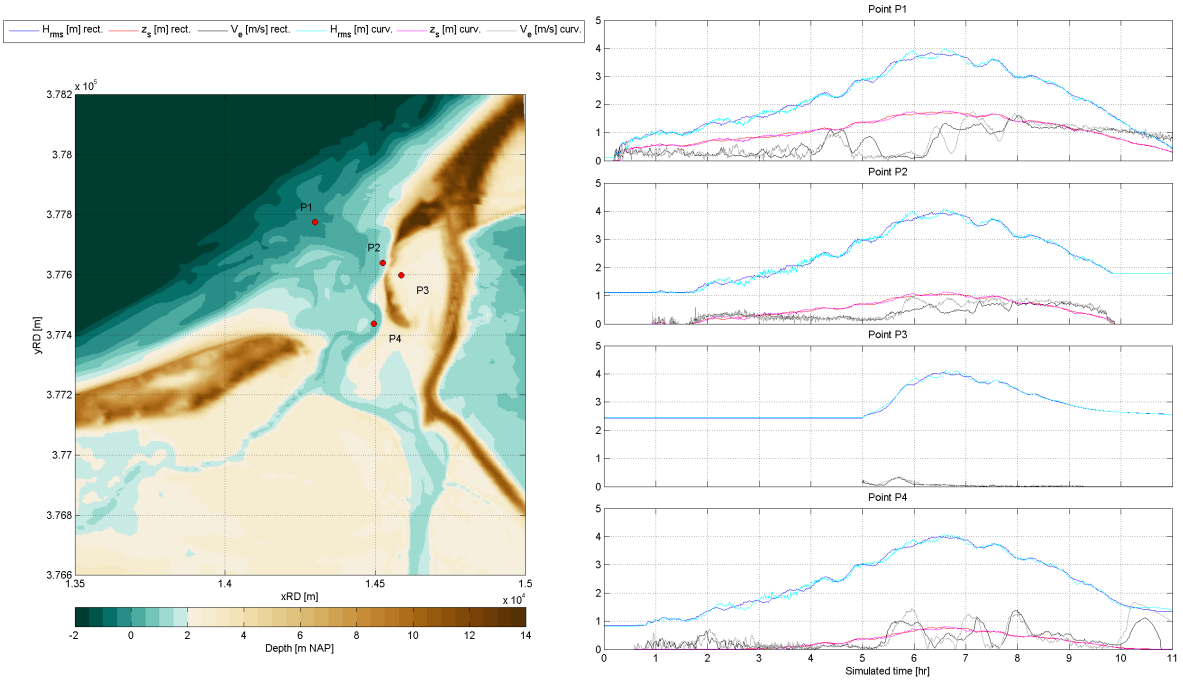

Figure 4.3: Curvilinear grid approach. Left panel shows the position of 4 locations around the Dutch dunes, whereas right panel shows the simulated time series at those points for both rectangular and curvilinear grids. Wave height is presented in blue and light blue, water level in red and magenta, and flow velocity in black and gray, respectively.

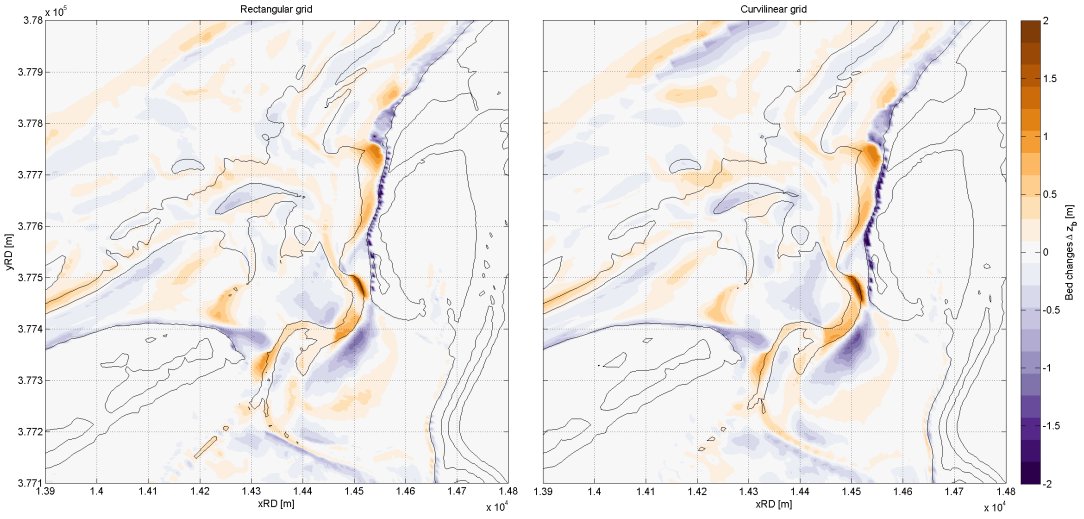

Figure 4.4: Curvilinear grid approach. Morphological impact is presented as the topography variations before and after the storm, for both rectangular (left panel) and curvilinear (right panel) grids. Warm colors indicate accretion whereas cold colors indicate erosion.

4.4.3. Offline coupling

As stated in section 4.2, most of the resources are employed by XBeach in solving the propagation of short waves. This is particularly problematic, for instance, when several runs using different options are wanted to be tested (as is normally the case during a hindcast calibration), since the same (long) computations are being repeated again and again in each run.

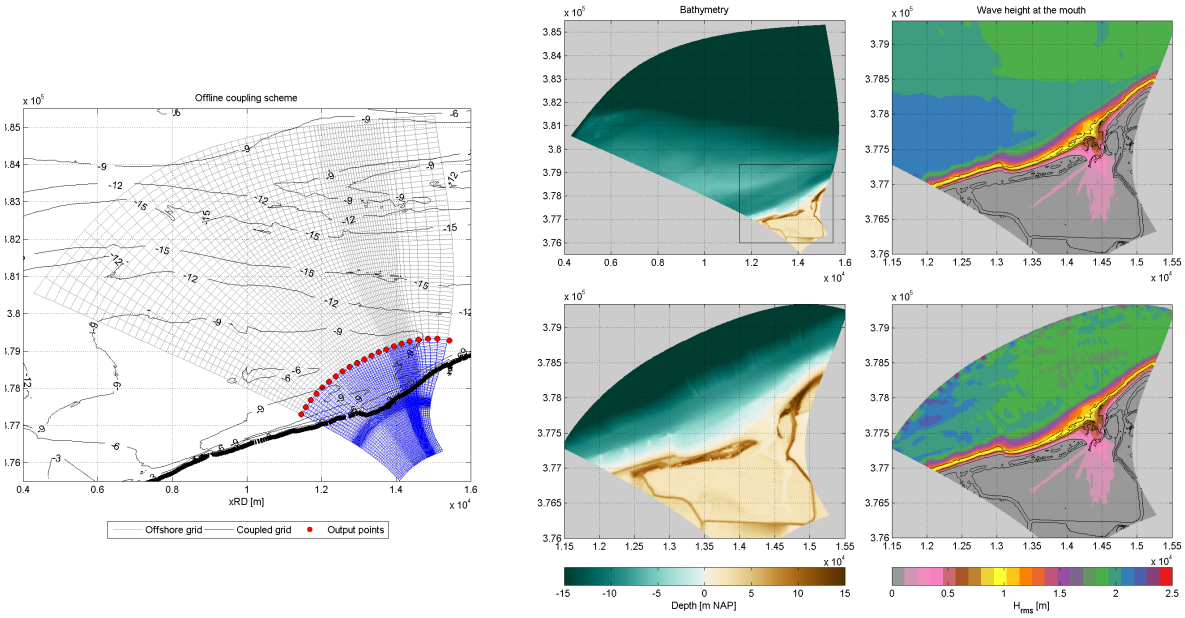

Figure 4.5: Offline coupling approach setup. Left panel schematically presents the full offshore grid, in gray, and the clipped coupled grid, in blue, along with the output points to perform the coupling. The middle column shows the bathymetry used in both grids (offshore upper panel, coupled lower panel), in which the deepening and smoothing of the bed level is observed for both. The right column presents the root mean squared wave height for both grids, zoomed at Het Zwin's mouth.

One way around this problem is to recognize that the hydrodynamics of the deeper parts of the domain will remain the same across different runs, and hence only need to be modelled once by a dedicated grid, and then use its results as forcing agents for a smaller and more refined grid, designed especially for morphodynamic computations. This approach was successfully followed by Dissanayake *et al.* (2014), who modelled the tidal flow and the propagation of a storm at Liverpool Bay using Delft3D and SWAN, respectively, and then using those results as inputs for an XBeach model to assess the morphological impact of the event. On a side note, both grids were made curvilinear, to follow the curved coastline of the site.

The coupling between the hydrodynamic and morphodynamic grids could be online or offline, the latter being favoured in this study, since the oceanographic conditions of the storm need to be computed only once.

In order to test the performance of this offline nesting scheme a new curvilinear grid—finer in the dune area—has been created. An XBeach run of the peak conditions of the storm (figure 4.1) has been performed, and the morphological impact has been computed. Additionally, the hydrodynamic conditions at several points located just offshore from the trench by the coast have been saved and used later as inputs for a smaller curvilinear grid. This coupled grid was actually created from the larger one, just by "clipping-off" the deeper cells.

The scheme of this offline coupling approach is presented in figure 4.5. The left panel shows both grids, labelled as *offshore* for the hydrodynamic grid, and *coupled* for the nested, morphodynamic one. These terms will be used indistinguishably here. As on the previous case, the deeper parts of the bathymetry have been flattened to a value of NAP-15 m in the offshore grid. The nested grid is relatively less deep, and thus it requires a bit more of work. From the deepest locations along the trench—which reaches NAP-10 m on average— a mild slope of 1/50 is projected offshore until a depth

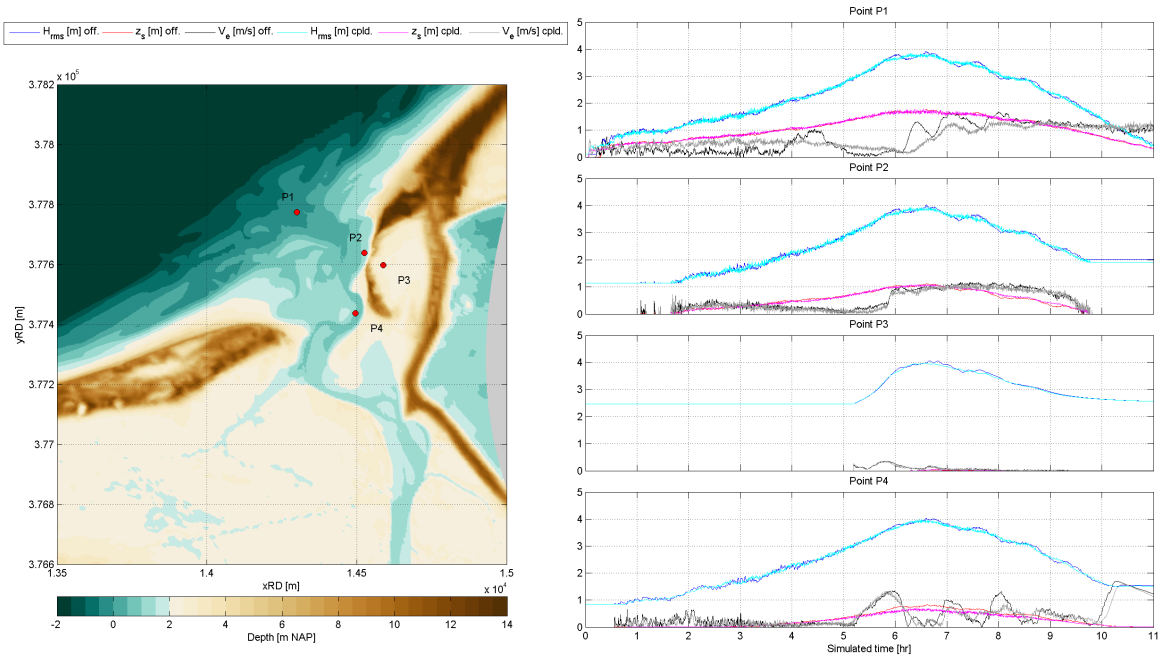

Figure 4.6: Offline coupling approach. Left panel shows the position of 4 locations around the Dutch dunes, whereas right panel shows the simulated time series at those points for both offshore and coupled grids. Wave height is presented in blue and light blue, water level in red and magenta, and flow velocity in black and gray, respectively.

of NAP-15 m is reached. The bathymetry of both grids is shown in the second column of the figure. As in the previous scheme, the comparison between the root mean squared wave height is fairly good. It appears that despite some differences in the deeper areas, both runs tend to be more similar within the surf zone, and at the mouth and within the estuary. This might be an indication that the breaking of waves is a dominant process in the inter-tidal areas.

As in the previous case, the agreement between the projected water levels, wave heights and flow velocities is very good at all analysed points, as shown in figure 4.6. The largest differences are observed in the velocity record, although the general trend is replicated in both cases. Additionally, it is noted that this new grid, with a resolution of $\Delta x \approx 4$ m at the dunes, does reproduce the overwash, or at least a part of it, since only a fraction of the storm was modelled.

This can be seen by the recording of wave heights behind the dunes in the times series, and the small washover fan observed in both simulations in figure 4.7. Little difference is observed between them, and considering that both discretizations were equivalent, these neglectable differences can only be assumed to be caused by the coupling scheme. Hence, the scheme seems to be a valid way to reduce the computational time, which was again reduced by more than half, since the nested grid had substantially less grid cells, as indicated in table 4.2.

Table 4.2: Offline coupling runtime.

	Offshore gird	**Nested grid**
nx	574	331
ny	324	324
runtime [hr]	52.2	19.9

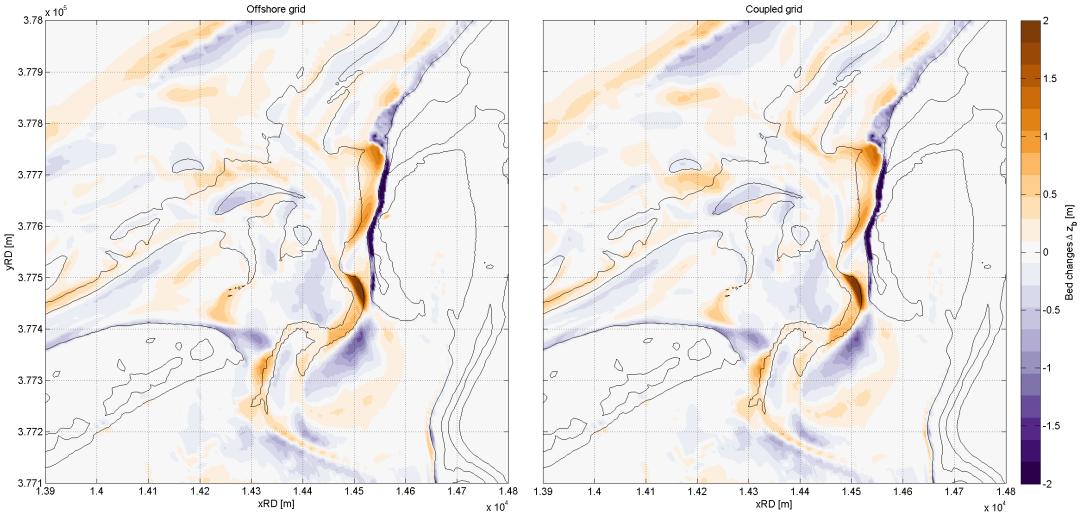

Figure 4.7: Offline coupling approach. Morphological impact is presented as the topography variations before and after the storm, for both offshore (left panel) and coupled (right panel) grids. Warm colors indicate accretion whereas cold colors indicate erosion.

4.5. Conclusions

Based on the analysed schemes, it is apparent that a great reduction in computation time can be achieved by using curvilinear grids over the more standard rectangular ones, without compromising the stability nor the accuracy of the computations. Additionally, it is decided to split the computations into two dedicated grids—a larger, coarser one to determine the hydrodynamic conditions of the storm, and a smaller, finer one to compute the morphological response of the dunes and the estuarine areas to these forcing agents.

Finally, the necessity of a very fine grid at the site of the overwash is remarked. The precise setup for the hindcast of the Sinterklaas storm at Het Zwin, which include these considerations, will be discussed in section 5.2.

5

Hindcast of the Sinterklaas storm

5.1. Introduction

Based on the schemes analysed on chapter 4, an optimized setup has been proposed to hindcast the Sinterklaas storm at Het Zwin. This chapter presents the setup of the model, its calibration process and the final results of the hindcast.

5.2. Model setup

5.2.1. Hydrodynamics

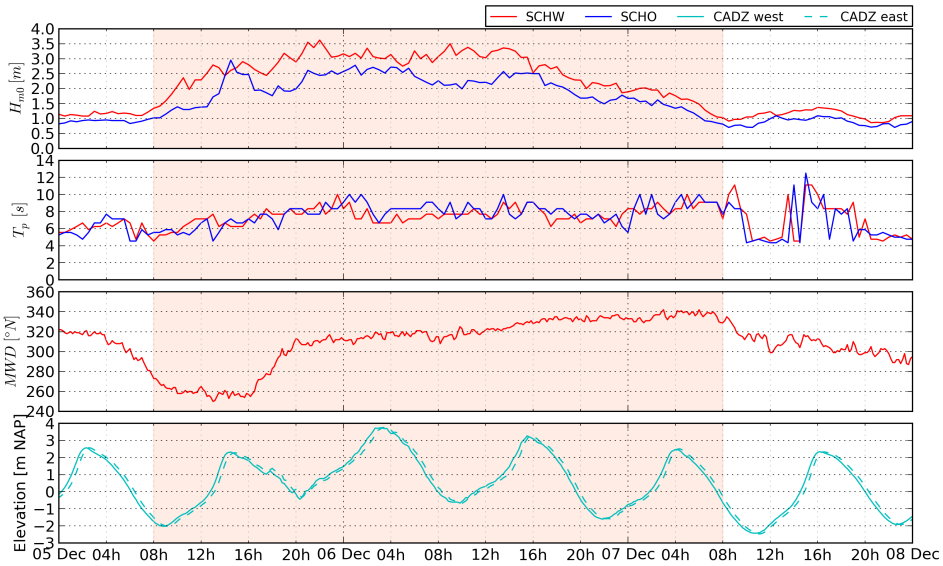

Figure 5.1: Hydrodynamic inputs for the wave grid. Significant wave height, peak wave period, and mean wave direction are presented in the first three top panles. Water level is shown in the lower panel. The color of each line indicates the location of the measurement. Highlighted is the modelled period.

In order to reproduce the wave field as accurately as possible, two buoy records are used here, namely the locations SCHW and SCHO (presented in figure 2.6), situated to the west and in front of the Zwin's mouth. The location of WIEL has been discarded considering that most waves arrived from the NW during the storm, thus waves recorded at this point are likely to hit the coast farther to the east of the mouth. Each location contains a record of wave height H_{m0} and peak period T_p every 30 minutes which have been used as input directly. The mean wave direction, MWD, however is only available for the

westernmost location, and is assumed to be representative for both. The wave records are presented in the three upper panels of figure 5.1.

No record is available for wave directional spread. A coefficient of $s = 10$ for the cosine spreading law has been assumed to be a representative value for this kind of storm.

The water level measured at the city of Cadzand was used as input (point CADZ). It showed slightly higher records than the other more offshore tide gauges. Since the horizontal tide is expected to be of importance in this area, also two different inputs, at each corner of the offshore boundary of the model, were needed. They were constructed based on an estimation of the time required for the tide to propagate along this boundary, made by a tidal Delft3D model of the region. The observed lag in water elevation between the point was $\approx$ 10 minutes.

The water level measured at CADZ was assumed to be representative of the easternmost boundary. In order the create the time series of the westernmost one, the record was separated between tide and surge, and the a new signal was built as the sum of the tide, leading ahead by 10 minutes, and the surge, at normal phase. The assumption behind this procedure is that the surge is a response to the wind forcing, acting on a large area, and affecting the whole project site at once, whereas the tide continues with its normal propagation.

The resulting forcing water levels are presented in the lower panel of figure 5.1, and the gradient they create is expected to drive lateral flow, simulating the horizontal tide. This is done in order to reproduce as accurately as possible all aspects of the hydrodynamic forcing of the storm, since it is hard to determine a priori their relative importance.

5.2.2. Topography

As in the analysis of the previous chapter, the deep bathymetry was obtained from the 2011 Vaklodingen dataset (Wiegman *et al.*, 2005), and the dunes and the estuary topography from the pre-storm lidar survey by the Vlaanderen government (EUROSENSE, 2013).

The data was used directly as it was, and no error analysis was undertaken (e.g. Plant *et al.*, 2002). Wherever the dataset overlapped, the most recent set was favoured.

5.2.3. Offline coupling scheme

Following the findings of the previous chapter (section 4.5) the modelling has been decided to be split into two parts, each with its own dedicated numerical grid and domain. First, the propagation of waves and determination of water levels and mean flow are computed in a hydrodynamic grid, whose results are used as inputs for a morphological grid in which several configurations will be run in order to assess the morphodynamics of the storm.

This offline coupling scheme is sketched in the left panel of figure 5.2. Again, for clarity sake, each drawn cell corresponds to 5 real cells in the numerical grid. The hydrodynamic grid as been extended offshore as far as to incorporate fully the shoal located between Het Zwin and the Zeebrugge port. The curvature of its offshore boundary assures that all waves used as inputs can reach the project site, and limited shadow zones are formed. The bathymetry beyond the shoal, in the offshore grid, is flatten out to a depth of NAP-15 m, as done before to noise in the generation of the bound long waves at the boundary of the domain.

The time series of hydrodynamic conditions are obtained at points located at the deepest positions on the beach trench, right in front of the Zwin's mouth, at an average depth of -10 [m NAP]. From those points offshore, the bathymetry of the nested grid is forced to follow a mild slope of $1/50$ up to a depth of -15 [m NAP], from where it remains constant. The employed bathymetries of both grids are presented in the right panels of figure 5.2.

Following this scheme allows to achieve workable runtimes. The hydrodynamic computations—which are only performed once in the offshore grid—take about one day to be completed, whereas the morphodynamic models run in a bit less than two days, as indicated in table 5.1, and they make use of 8 CPU cores for each run. Moreover, several morphodynamic runs can be carried out simultaneously

Table 5.1: Offline coupling runtime.

	Hydrodynamic (offshore) gird	**Morphodynamic (nested) grid**
nx	244	363
ny	244	399
runtime [hr]	23.7	37.6

at the Linux cluster of Deltares, which allows to complete 5 model runs in less than two days (three if the hydrodynamic run is also taken into account).

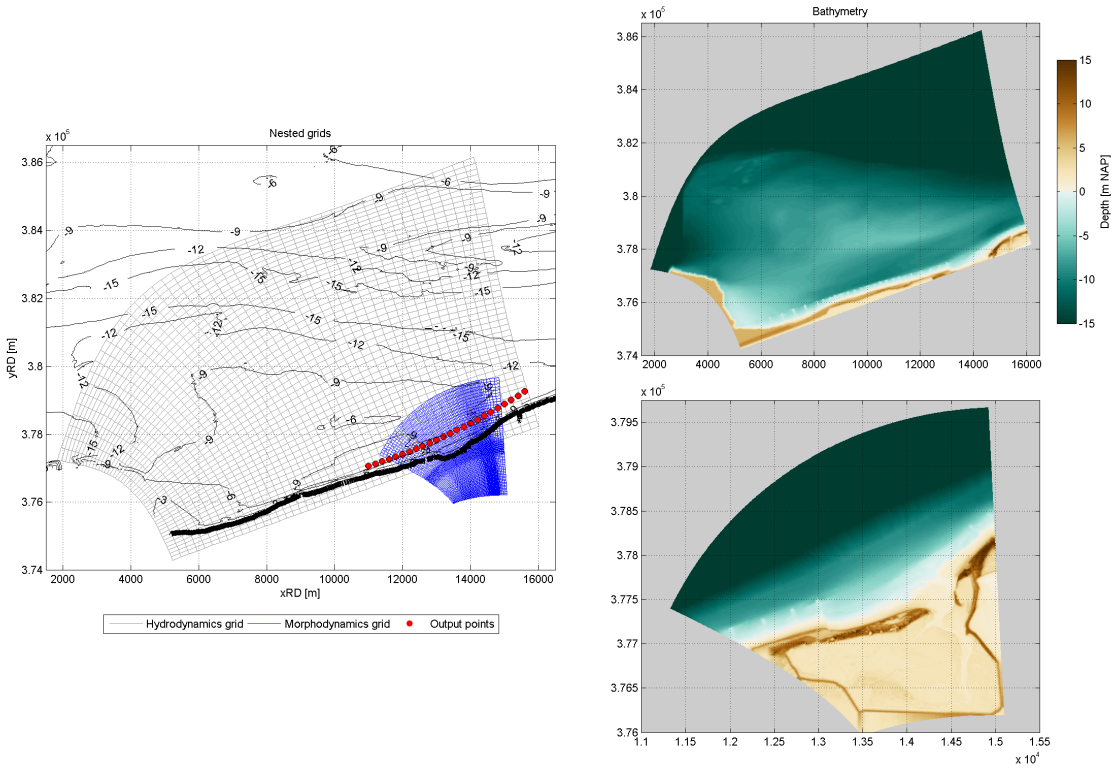

Figure 5.2: Nesting scheme for offline coupling. Left panel shows the offshore (gray) and nested (blue) grids used for hydrodynamic and morphodynamic computations, respectively, over the measured bathymetry. The output points for the nesting, which lie along the a nearshore trench, are indicated in red. The left column presents the actual bathymetry used in both grids (hydrodynamic in upper panel, and nested in lower panel).

The nested grid has higher resolution at the site where overwash is expected, as compared to the grids used in the previous assessments, with a grid size of $\Delta x \approx 3$ m. The time series used for wave transfer are showed in figure 5.3, in which wave output locations are numbered from west to east, and coloured from red to blue. In the background the wave time series used in the offshore grid are also plot, following the same color scheme. This makes clear the influence of the shoal in reducing and refracting the waves, especially at the beginning of the storm when wave directions were mainly from the west.

5.3. Calibration

It is good practice to calibrate a model before producing any forecast, in order to increase its reliability. Particularly, XBeach has a wide set of modifiable parameters which might render the calibration an even more challenging task, as it already is. All of these parameters—some physical, some numerical—have a predefined default value, and Deltares works constantly in finding the best set of default values. The most sensitive parameters of the 1D XBeach model have been found by van Geer *et al.* (2014),

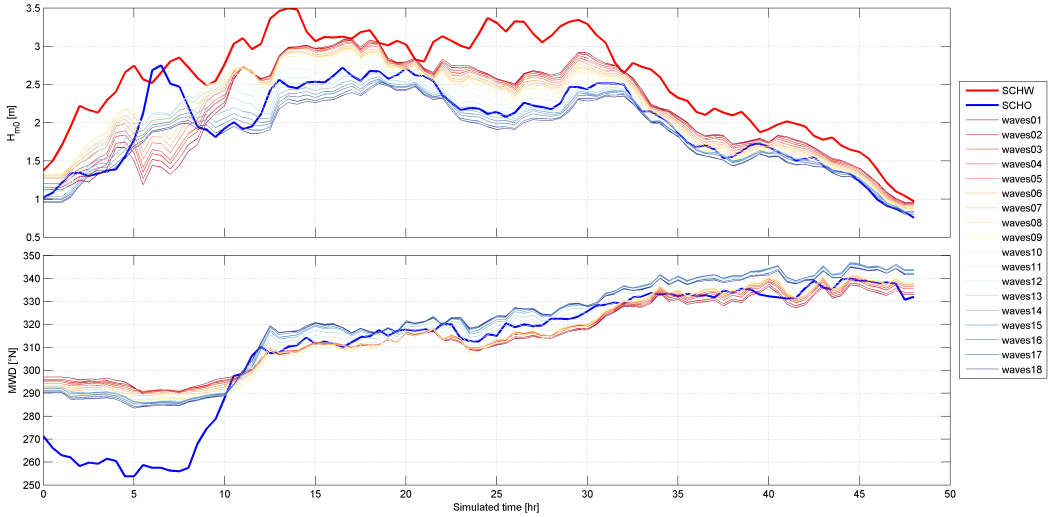

Figure 5.3: Time series of wave height (upper panel) and mean direction (lower panel). Inputs are indicated in thick lines, while records at the coupling points are presented in thinner lines. All time series are color-coded from red (west) to blue (east).

who systemically changed its setup and compared the results against a test-bank composed by lab experiments and field measurements. The list of these sensitive parameters is presented in table 5.2, along with their default value on XBeach and the new proposed values found to fit best the calibrated cases.

Table 5.2: Most sensible parameters for XBeach 1D and their recommended values.

Parameter	Default value	WTI settings
`C`	57.2	99.0
`gammax`	2.00	2.364
`beta`	0.10	0.138
`wetslp`	0.30	0.260
`alpha`	1.00	1.262
`facSk`	0.10	0.375
`facAs`	0.10	0.123
`gamma`	0.55	0.541

The list can be viewed as a combination between physical properties of the beach to be modelled—bed friction, `C`, critical beach slopes for avalanching in wet condition, `wetslp`, and short-wave-induced onshore transport, `facSk` and `facAs`—and the numerical parameters that control the way in which XBeach models the physics. It is interesting that most of the sensitive parameters are related with the wave breaking algorithm—`alpha`, `gamma`, and `gammax`—which highlights the relative importance of the correct determination of the short-wave density spectrum.

XBeach's complex breaking algorithm has been extensively tested and calibrated, and despite the fact that modifying its parameters might greatly affect the model's output, its behaviour will not be analysed on this work, nor its parameters will be used to calibrate the hindcast of the Sinterklaas storm. A few thoughts about this decision are presented in section 7.3, on the discussion chapter.

Instead, the focus of this thesis will remain on the physical properties of the beach, whose correct estimation appears to influence greatly the accuracy and reliability of the model's output. It is reassuring the see that both parameters used by de Vet *et al.* (2015) to calibrate their model are present on the list: the bottom friction, and the `facua` parameter, which controls both the asymmetry `facAs` and the skewness `facSk` factors (although they can, actually, be set separately). The recommended values

for this parameters are in line with the train of thought of de Vet *et al.* and Nederhoff *et al.* only for the `facua` factor (i.e. increasing its value), but against it for the bottom roughness, which is advised to be lowered (i.e. a higher Chezy coefficient). This difference might be due to the 1D nature of the calibration, or the absence of overwash in the test-bank.

The other property indicated as relevant (at least in 1D cases) is the wet critical slope of the dune, which has been considered a less sensitive parameter by de Vet *et al.* and Nederhoff *et al.* in their calibrations. Its effect will be investigated in this thesis.

The calibration procedure will follow the proposed two-step process: first calibrate the `facua` coefficient under collision regime in the Belgian dunes, and later use that value to calibrate the Chezy coefficient `C` that best fits the observed overwash fan. Once both parameters are set, the influence of the parameters for avalanching is tested.

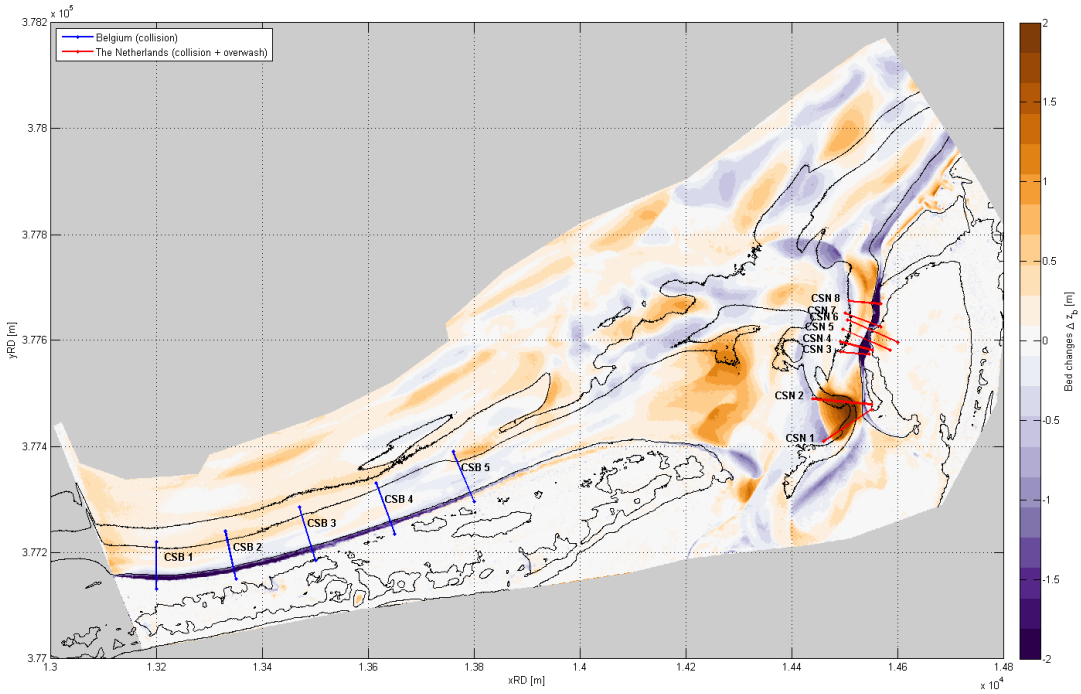

Figure 5.4: Cross sections used for calibration shown over the topographic changes due to the storm, as observed in the lidar data. Sections are labelled CSB for the Belgian dunes, and CSN for the Dutch dunes.

In order to compare different model runs, it is necessary to define and use a certain metric which can quantify the result, i.e. how far away from the observed morphological changes is each model output. In recent years, the use of the Brier Skill Score (BSS) has become a widespread used metric in morphodynamic modelling (Sutherland *et al.*, 2004). It intends to measure the amount improvement of the morphological prediction in comparison with some base prediction, normally the initial state of the system.

The idea of model skill is to have an indicator of how good a model is in only one figure (with 1 being a perfect score, 0 corresponding to the base prediction, and any negative value a worst prediction than that) can be very handy, specially when the modelling comprises several complex phenomena, as is the case in morphodynamic modelling. Moreover, the BSS would present attractive features: it is non-dimensional, hence comparable among different cases and scenarios, it corresponds with the judgement or expectation of experts, and can be decomposed between phase and amplitude components.

These characteristics explain, in part, the success the BSS has had in being adopted as a model metric. However, recent criticism has arisen which is calling to a critical review of the skill score. Particularly Bosboom *et al.* (2014) have shown that the BSS tends to reward predictions that underestimate variability, since it doesn't distinguish between the different length scales of the processes. They also

criticised the use of the initial state as a base prediction (especially in cases where cyclic behaviour is expected), and most notably they argued that, actually the BSS does not match the experts' judgement, in many cases.

Given all this controversy, the questioned Brier Skill Score will not be used as metric in this thesis. Instead, the volume of sand lost above high water level will be employed (at it was by van Geer *et al.*, 2014), since it corresponds to a sensible physical indicator, easy to grasp, visualize and compare between the model runs. Moreover, the loss of dune mass appears to be a valid metric for storm assessment, from a coastal management point of view.

Figure 5.4 shows the locations of several cross sections drawn along the Belgian and Dutch coasts near the mouth of Het Zwin. These sections are used during the calibration, by computing the lost volume due to the storm as observed in the lidar data, and then comparing them against the different model outputs.

Finally, special attention is given to the *expert's judgement* in this calibration process, since there seems to be an agreement on its relevance, despite the facts that it is poorly defined and hardly measurable. This soft, qualitative skill of the modeller can be thought as his or her capacity to estimate the physical meaningfulness and/or the likeliness of a certain prediction, based on the knowledge of the involved physical processes and previous experiences. In all honesty, it is mostly used to rule out results that "don't make sense".

5.3.1. Short-wave induced onshore transport

Several values for the wave asymmetry and skewness transport `facua` where tested, ranging from 0.1 up to 0.35, with a larger onshore transport as the parameter increases. Measured profiles, before and after the storm, at the aforementioned cross-sections are presented in 5.5a for the Belgian dunes, and 5.5b for the Dutch dunes. The volume of sand lost during the storm is highlighted between both curves. On top of these curves, the final topography of each model run has been drawn in order to show the influence and this transport parameter.

A negative correlation between the `facua` parameter and the lost volume is clearly observed. This might be explained by the extra stability given to the toe of the dunes by the larger flow of sand transported by waves, which seems to hinder the avalanching process. This trend is observed for both, collision and overwash regimes. As a trend, the deposition slopes as computed by the model tend to be milder compared with the measurements, whereas the scarping slopes in the model seem to be steeper than the observed ones.

The root mean squared error (RMSE) of the estimation of the losses volume is presented in table 5.3, for each stretch of coastline and for both combined. A value of `facua` = 0.15, slightly higher than the default one, minimize this error under collision regime. However, the slopes in the upper part of the dunes are better represented by the model using `facua` = 0.10, and the error decrease is relatively small compared with the large deviations observed for larger `facua` values. In short, both values, 0.10 and 0.15, show fairly similar results, with the first giving profiles which are thought to be more representative of the dune erosion.

Hence, the onshore transport by asymmetry and skewness of short waves, which is thought to control the collision regime, has been found to produce the best fit with a value of `facua` = 0.10, which corresponds with its default value. This is coherent with the experimental determination of the `facua` coefficient along the Holland coast, which has been found to have similar values.

Table 5.3: RMSE on dune erosion volumes above high water, as function of `facua`. The smallest and largest errors per row are indicated by green and red colours, respectively.

`facua`	**0.10**	**0.15**	**0.20**	**0.25**	**0.30**	**0.35**
Belgium RMSE	4.3	3.8	7.7	13.9	16.7	18.7
Netherlands RMSE	25.6	25.6	26.0	26.2	26.8	30.2
Overall RMSE	18.3	18.3	19.2	21.0	22.3	25.1

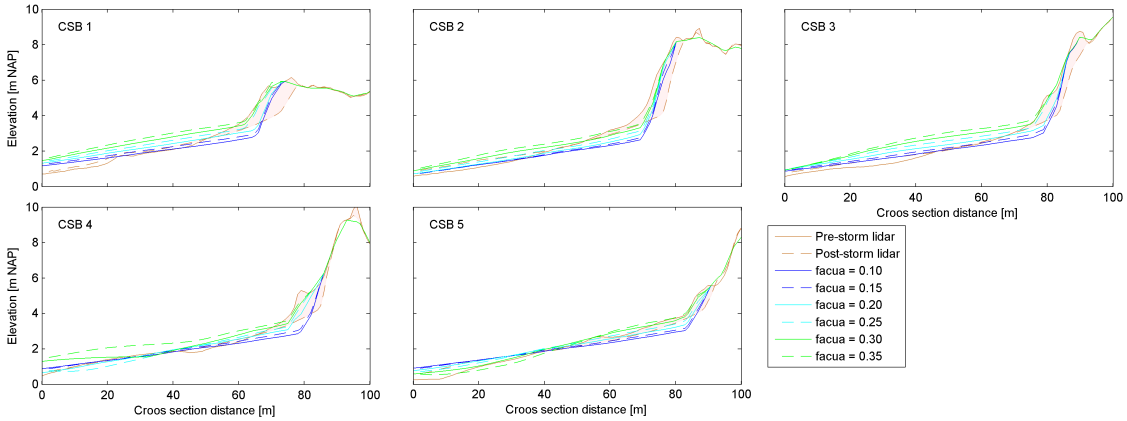

(a) Belgian dunes.

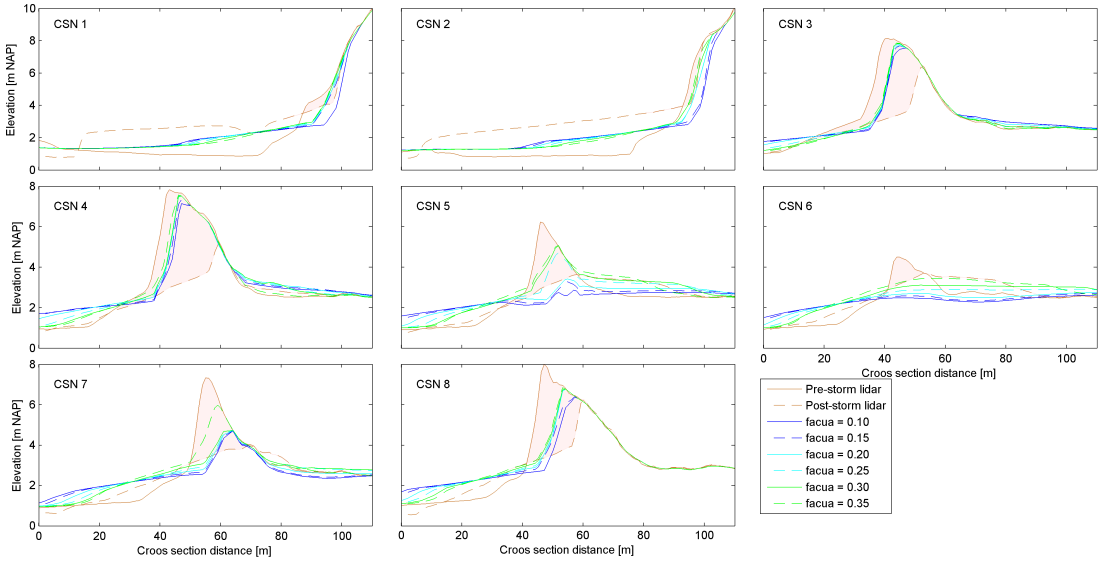

(b) Dutch dunes.

Figure 5.5: Calibration of onshore transport `facua`.

5.3.2. Bottom roughness

Bed friction is a complex and recurrent topic in hydraulic engineering, which tends to be addressed in a macro-scale and averaged way, discarding the details of skin and form friction, turbulent boundary layer and vertical distributions of viscosity and velocities. The main reason to do this is because it works, in the macro-scale, as the usage of the Chezy or Manning formulae has shown.

Despite this broad representation of the bottom friction, it is easy to grasp that some parts of the dune barriers must be rougher—as in they exert more opposition to the flow—than others. Particularly, it is expected that all terrain above the inter-tidal area will be rougher, since they will not be "washed-out" in every tidal cycle. Moreover, these areas are prone to develop vegetation and to concentrate debris, which will further difficult the flow of water.

Once the `facua` has been set to 0.10, several runs were carried out varying the bed roughness, represented in this case by the Chezy coefficient `C`. The bottom friction was first varied in the whole domain ranging from 25 to 55, and later increased only above the high water level, assuming that the default value is representative of the inter-tidal area. Two higher frictions were tested, 25 and 35, for two different high water levels, 2.0 and 2.5 [m NAP].

The computed bed level changes are presented in figure 5.6. In the upper row the bed has been made increasingly rough form left to right. It is clear that the morphological impact of the storm decreases with increasing bottom friction. Thus, despite the fact that the overwash fan is better reproduced with a higher friction (lowest Chezy coefficient), it does not seem advisable to modify this parameter all over the domain.

The lower row shows the topographic changes for frictions maps that consider the default roughness, `C` = 55, below high water level and a higher roughness above that datum. It is clear across the four panels that the impact below high water level is not sensitive to this increase in friction on the upper dunes, which is expectable and desirable. It is also apparent that a value of `C` = 35 is not rough enough as to contain the washover fan inside the "shell-type" form observed in the measurements.

Hence a bed friction coefficient of `C` = 25 above high water level has been found to give the best fit between the computed and the observed washover fan shape. The position of this vertical limit was found to be $z_b = 2.0$ [m NAP], for which the shape of the fan is the most symmetric, as measured.

Just for completeness, the associated computed erosion volumes are presented in table 5.4, although they were not used in the calibration process. It is interesting to see that the variation on the dune damage are relatively small across different roughness, which supports the assumption that friction is more relevant for overwash than for collision regime. Nonetheless, it is also clear that the smaller errors are observed for the better estimates of the friction parameter.

Table 5.4: RMSE on dune erosion volumes above high water, as function of `C`.

C	55	45	35	25	35@2.5	35@2.0	25@2.5	25@2.0
Belgium RMSE	4.3	3.9	3.6	6.3	3.5	2.8	2.9	2.3
Netherlands RMSE	25.6	25.9	24.4	26.2	24.8	24.6	24.4	25.5
Overall RMSE	18.3	18.5	17.4	19.0	17.7	17.5	17.4	18.1

5.3.3. Critical slopes for avalanching

So far the calibration has followed the two-step scheme by de Vet *et al.*, however the model consistently underestimates the erosion volumes, especially in the dunes around the gap where the overwash took place. This is likely to be related to an underestimation of the avalanching process, which is a dominant process for eroding the higher parts of the dunes. This can be explained by two complementary factors: the critical slopes might be too steep, and the grid discretization might be forcing a milder-than-real slope on the model. Only the first aspect will be treated in this section.

Both the wet and dry critical slopes were varied to values of 0.25 and 0.20, for the first, and 1.00 and 0.85, for the latter. Their effect on the final profiles is presented in figure 5.7a for the Belgian

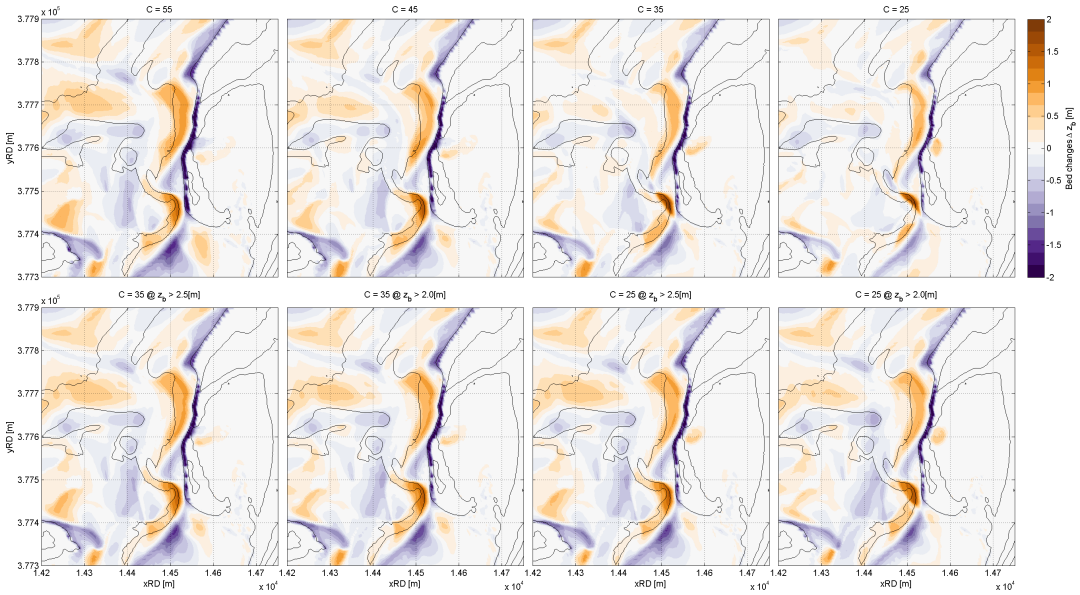

Figure 5.6: Calibration of bottom roughness. Upper row shows smaller topographic changes as the bottom becomes rougher. Lower panel shows the effect on the fan shape of increasing the bed roughness only at the top of the dunes.

dunes, and figure 5.7b for the Dutch ones. It is clear that the results are less sensitive to changes in the dry slope. In contrast, changing the wet slope to a milder value modified the observed slopes on the cross-sections, making them more similar to the observed ones. Particularly, a smaller value of `wetslp` increases the eroded volume in the dunes around the gap, where the model shows the largest underestimation.

It the figure it is also noticeable that the model reproduces accurately the cross-section of the washover fan, which is slightly better estimated with the lowest values of the critical slopes, i.e. `wetslp` = 0.20 and `dryslp` = 0.85, which are also the ones which minimize the lost volume from the dunes.

Table 5.5: RMSE on dune erosion volumes above high water, as function of `wetslp` and `dryslp`.

wetslp	**0.30**	**0.25**	**0.20**	**0.25**	**0.20**
dryslp	**1.00**	**1.00**	**1.00**	**0.85**	**0.85**
Belgium RMSE	2.3	2.2	2.6	2.1	2.6
Netherlands RMSE	25.5	21.5	18.5	20.7	18.3
Overall RMSE	18.1	15.3	13.2	14.7	13.1

5.3.4. Optimal settings

Summarizing, the root mean squared error of the volume of lost sand above high water level, in several cross-sections, has been used as the metric to calibrate the hindcast of the Sinterklaas storm at Het Zwin. The procedure consisted in calibrate first the effect of onshore transport due to short waves asymmetry and skewness on the dunes under collision regime, determined by the `facua` parameter, and later use that value to calibrate the roughness of the higher parts of the dunes, above high water level. Additionally, it was shown that the hindcast could be improved by reducing the critical slopes for avalanching.

The best set of parameters, for this particular case, is presented in table 5.6, and the computed topographic changes obtained using these parameters is shown in figure 5.8, along with the measured changes.

About the best set of parameters, it is fair to state that probably the use of `facua` = 0.15, and/or

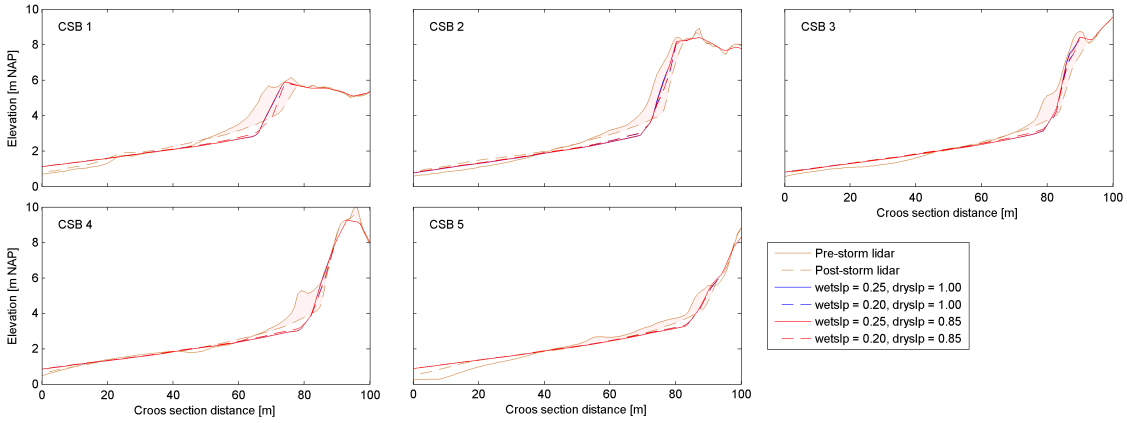

(a) Belgian dunes.

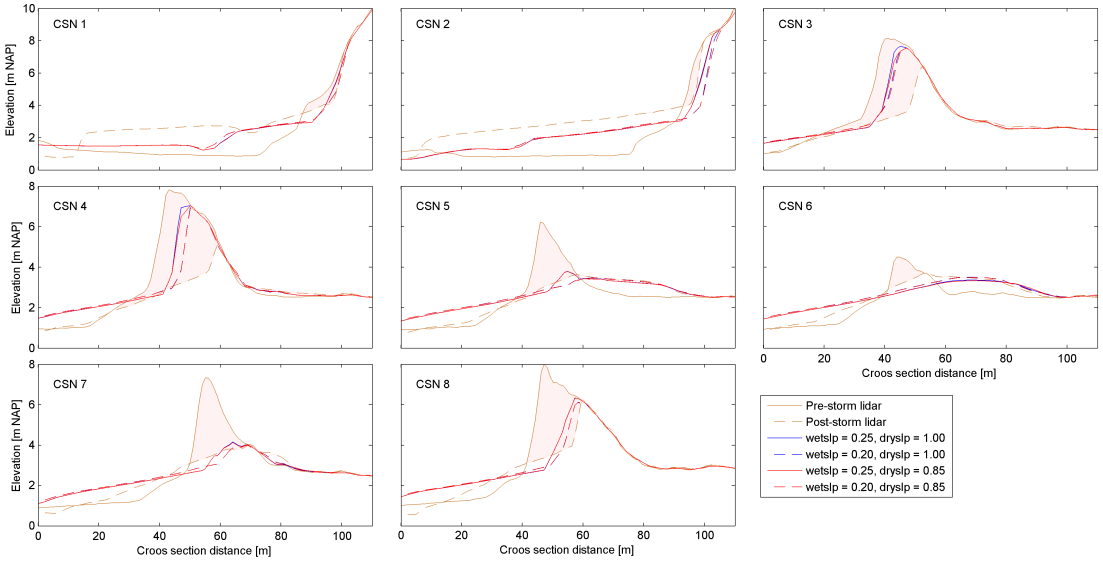

(b) Dutch dunes.

Figure 5.7: Calibration of critical slopes for avalanching.

Table 5.6: Calibrated set of parameters.

Parameter	Calibrated value
facua	0.10
C below 2.0 [m NAP]	55
C above 2.0 [m NAP]	25
wetslp	0.20
dryslp	0.85
morfac	1

dryslope = 1 might be nonetheless valid options, since their sensitivity of the outputs was small within that range. It is also remarked that this best set of parameters was obtained using a morphological accelerator factor of morfac = 1, i.e. without acceleration of the hydrodynamic inputs. The dependency of the calibration parameters on this factor will be conceptually analysed in section 7.4 of the discussion chapter.

Finally, a good agreement between the measurements and the model is achieved, which is satisfactory for an overwash event modelling. However, some discrepancies still exist, most notably the spit formation at the tip of the Belgian side and the shift on the channel position, which are not well captured by the model.

Considering that the most uncertain input used for the modelling corresponds to the initial bathymetry, which was measured seven months prior to the storm, the first attempt to improve the hindcast should include a better estimate of the topography at the beginning of the storm, which could be achieved if new measured data would become available (not very likely), or by performing a numerical morphodynamic of the long-term evolution of the system—both alternatives outside the scope of this thesis. Only then it would be possible to investigate if XBeach is in fact missing some relevant physics that could explain the observed differences.

5.4. Sensitivities

Once the best fit of the hindcast of the Sinterklaas storm has been found, a few parameters were varied in order to gain insight on their influence over the results. The analysed cases comprised the inclusion of wind, the removal of the time lag from the time series of tide used as input, and the refinement of the numerical grid.

5.4.1. Wind

In XBeach the effect of the wind is taken into account only as a shear stress in the momentum equations, acting on the water surface. Hence, the generation and growth of sea waves is not included (which could arguably be important on large domains).

In order to test the relevance of the wind action, a sensitivity run was setup considering a constant wind of 15 m/s of velocity, with a direction of 300°N, which is representative of the peak of the storm, when most of the erosion took place.

The inclusion of wind did not produce significant differences in the hindcast, hence wind is considered to be less significant that the oceanographic forcers, like tide and waves.

5.4.2. Horizontal tide

The inclusion of a time difference on the tide time series was intended to include tidal flows, which might be of importance on the project site, located in the "deltaic" region of The Netherlands. In order to test this assumption the time lag has been removed, i.e. the same time series of water elevation—including

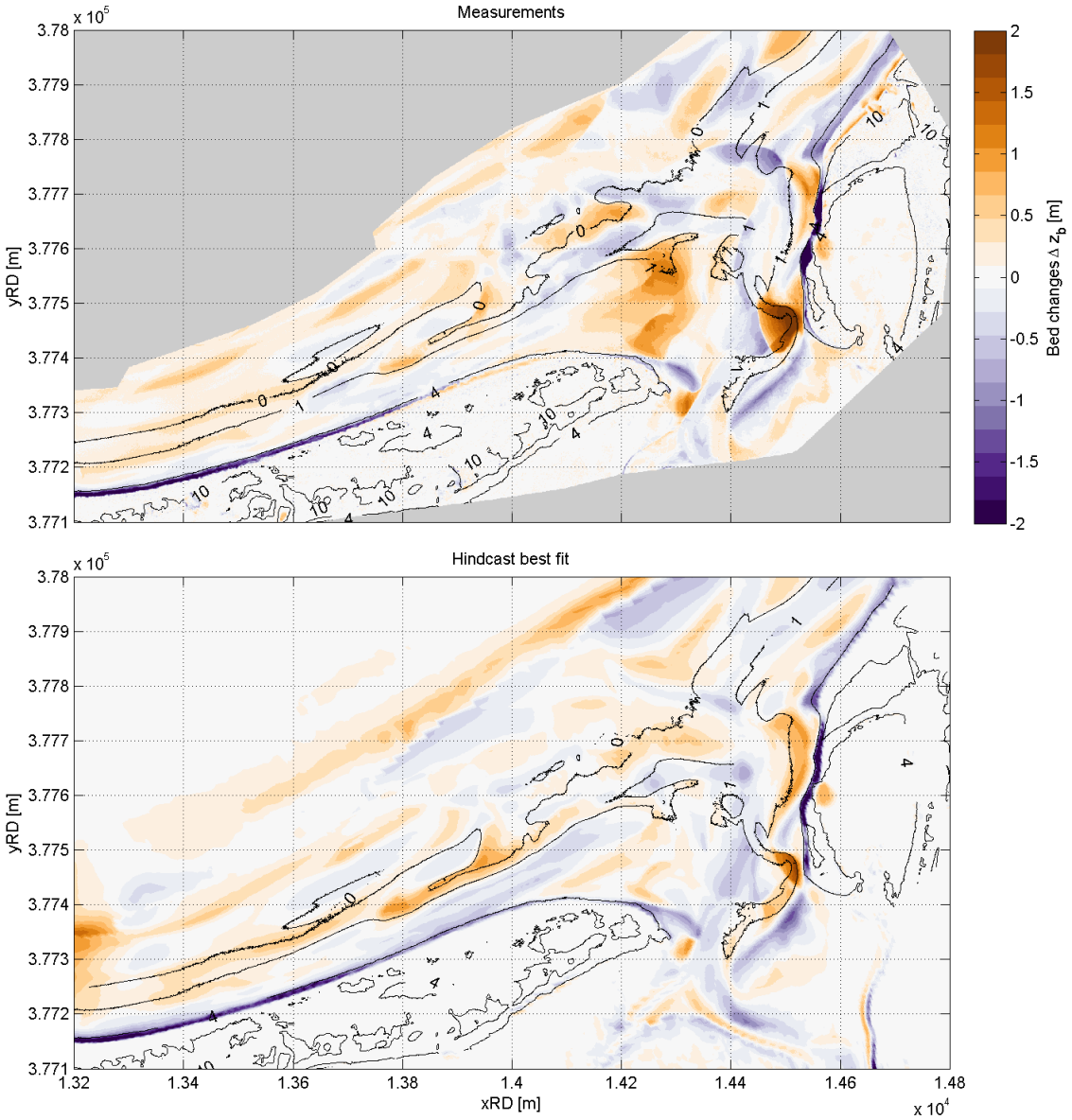

Figure 5.8: Morphological impact of the Sinterklaas storm as recorded by the lidar data (upper panel), and as modelled with the best set of parameters (lower panel). Scarping (dune erosion) is observed at both dune fields (Belgian and Dutch), with the volume of sand lost being significantly larger around overwash location. Most of the eroded sediment from this location is deposited downdrift into the tidal channel, although the model seems to slightly underestimate its volume. The washover fan shows a rather circular shape, and is confined to the vicinity of the overwash location. A relatively large sand spit at the end of the Belgian side is observed only in the measurements, but not in the model, which might indicate longer-term effects as a cause rather than the storm.

the astronomical tide and the storm surge—has been applied at both ends of the offshore boundary of the domain, thus no tidal flow is expected.

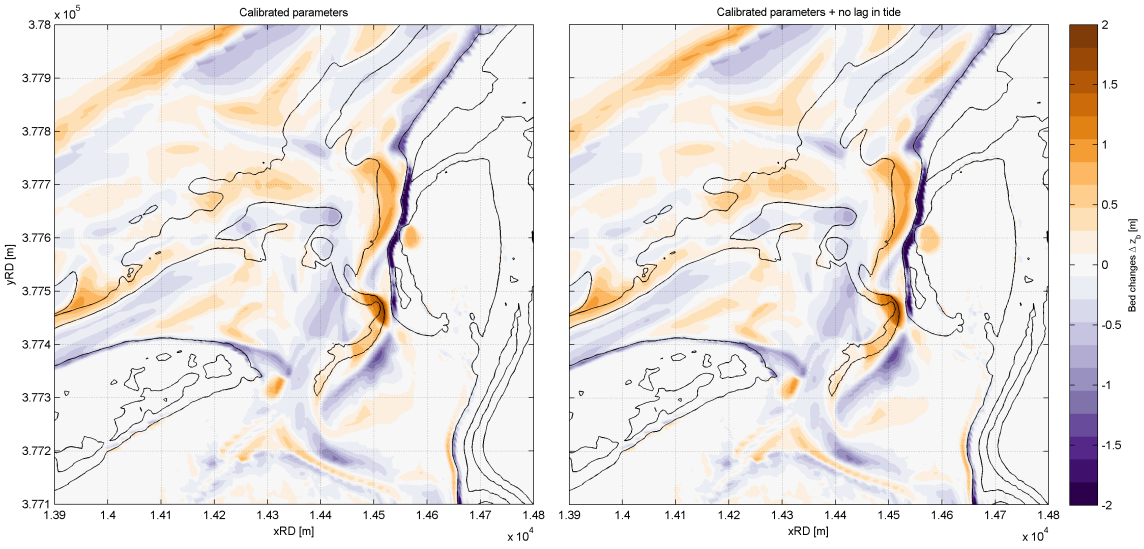

Figure 5.9: Effect of the time lag of tide input over morphological changes.

The impact of this change on the predicted morphological changes is relatively small, as shown in figure 5.9. It can be noted, nonetheless, that the volume of dune erosion is increased as well as the size of the washover fan. It would appear that the more "direct" attack of the storm causes more damage to the dunes, compared against a situation where there is alongshore flow, which might hinder the volume of water overflowing the dunes, and might refract more the wave field.

It is, however, impossible to determine which approach is more representative of the actual conditions during the storm, since no oceanographic measurements of velocities at the site were taken (as is usual in stormy events in remote locations).

If the objective is to reproduce accurately past conditions, perhaps the modeller should make the effort and use the most realistic conditions available—reducing the hydrodynamic uncertainties—and use the more calibrated, and validated available transport formulations he or she can dispose of. In this sense, the inclusion of the horizontal tide is advisable.

5.4.3. Spatial discretization

Finally, a run with refined grid (double resolution) was carried out in order to assess the sensitivity of the results to that variable. Figure 5.10a shows the dune profiles, obtained with the original and refined grids, at the previously defined cross-sections on the Belgian side, and figure 5.10b the ones on the Dutch side.

The improvement on the prediction of the profile after the storm is apparent, especially for the upper part of the dunes, at both sides of the runoff channel. However, the model systematically tends to locate the new toe of the dunes below the observed level, which tend to increase the error made in the Belgian side. Part of the extra sediment made available is deposited on the washover fan, making it slightly thicker, although its position is still well represented.

The errors on the eroded volumes from the dunes are presented in table 5.7. It is clear that the overall error is reduced when using a finer grid, despite the overestimation made in the dunes under collision regime. This better result is largely explained by the better approximation of the large dunes eroded around the overflown dunes, where avalanching is expected to be the dominant erosion process.

However, the runtime for this finer model was too large, 3.6 days, which makes it not suitable for engineering purposes. It could be argued that the increase on the quality of the prediction—model

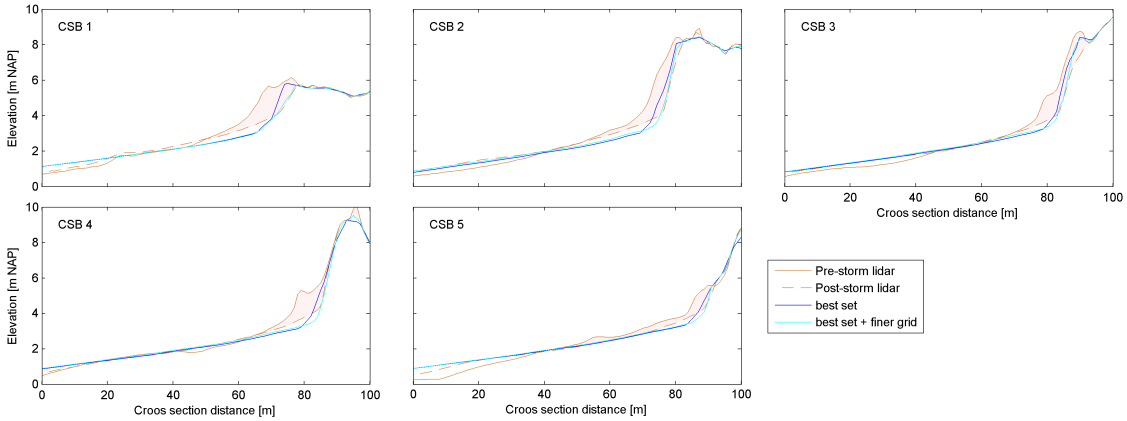

(a) Belgian dunes.

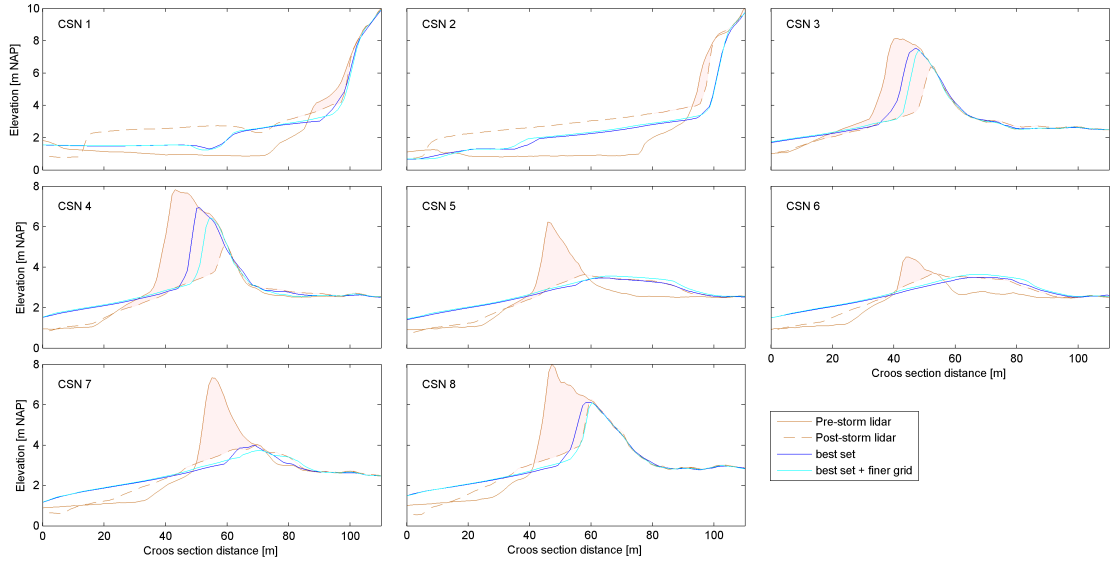

(b) Dutch dunes.

Figure 5.10: Improvement on predicted profiles with increasing resolution.

skill if you prefer—is marginal, compared to the cost of that improvement. In other words, the original model was already good enough and the gain in accuracy by a finer grid is not worth the cost.

Table 5.7: RMSE on dune erosion volumes above high water, as function of the grid resolution.

Grid	**Original**	**Refined**
$\approx \Delta x$	**3.0**	**1.5**
Belgium RMSE	2.6	4.7
Netherlands RMSE	18.3	12.9
Overall RMSE	13.1	9.7
Runtime [hr]	37.6	88.5

Finally, the question of whether the calibrated parameters are also the best parameters for a finer (or coarser) grid arises—or remains. In other words: are the parameters, like the critical slopes for avalanching, a function of the grid resolution? This question lies largely beyond the scope of this thesis. However, it is fairly easy to realize that the maximum slopes that the model can perceive do depend on its cell size, in a similar fashion as how the propagation speed of the waves also depends on it.

For the time being, the use of calibrated parameters on a finer will be regarded as a fair approximation, given the fact that a calibration procedure on this finer grid does not seem feasible in a reasonable amount of time.

6

Scenario analysis

The calibrated model was used to assess two interesting hypothetical scenarios: the influence of the runoff channel position over the safety of the Dutch dunes, and the expected impact of a fairly large event—the normative storm.

6.1. Maintenance problem

As stated in subsection 2.1.2, the tidal channel at the mouth of Het Zwin normally migrates towards the Dutch side of the estuary, and is regularly dredged to keep it in place. The problem of how often, or under which conditions this maintenance dredging should be carried out is relevant for the responsible waterboard, but lies beyond the scope of this work and will not be addressed here.

However, it is possible to simulate the storm should the position of the runoff channel would have been the one recorded in the 2014 lidar campaign (Hansa Luftbild/TopScan, 2014). The main differences between this hypothetical run and the previously determined best fit are the inclusion of the sand spit at the mouth of the estuary on the Belgian side, and a more straight channel located nearer the Dutch dunes.

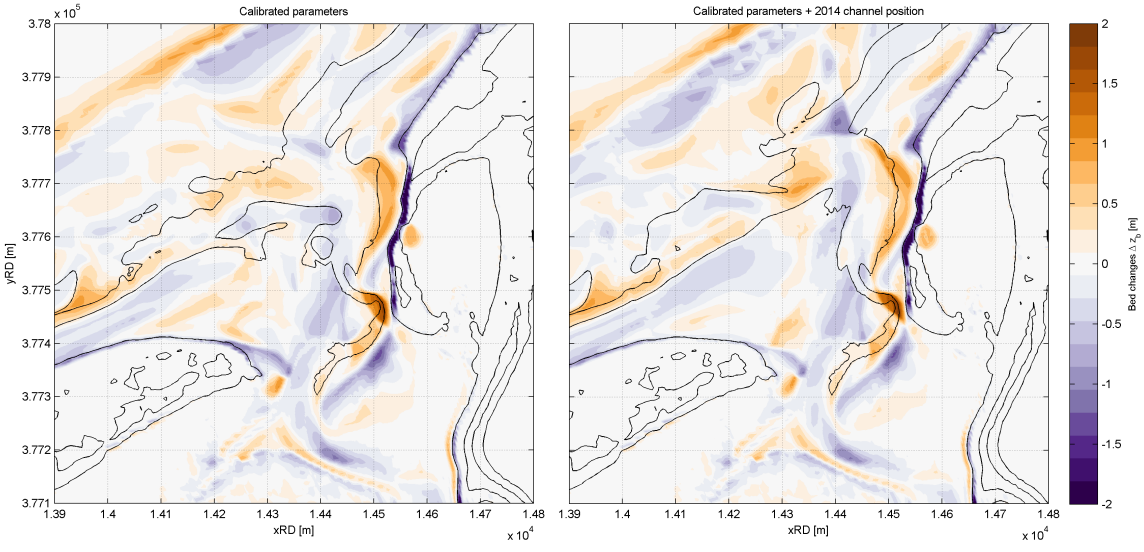

Figure 6.1: Effect of the sand spit and channel position over the morphological changes.

Figure 6.1 presents a comparison between the predictions of both models. The initial bathymetry for each run is indicated by the countour levels: 0, 1, 4, and 10 [m NAP]. It is clear that no dramatic

differences are observed, which might indicate that the position of the channel does not determine a big change in the hydrodynamic conditions at the Dutch dunes, at least in this analysed case.

However, some differences are evident, particularly a slightly higher erosion of the dunes' front—which might be explained by focusing of the wave action—and different deposition patterns along the tidal channel, given its different shape.

In short, the position of the tidal channel does not seem to greatly influence the erosion of the Dutch dunes.

6.2. Normative storm

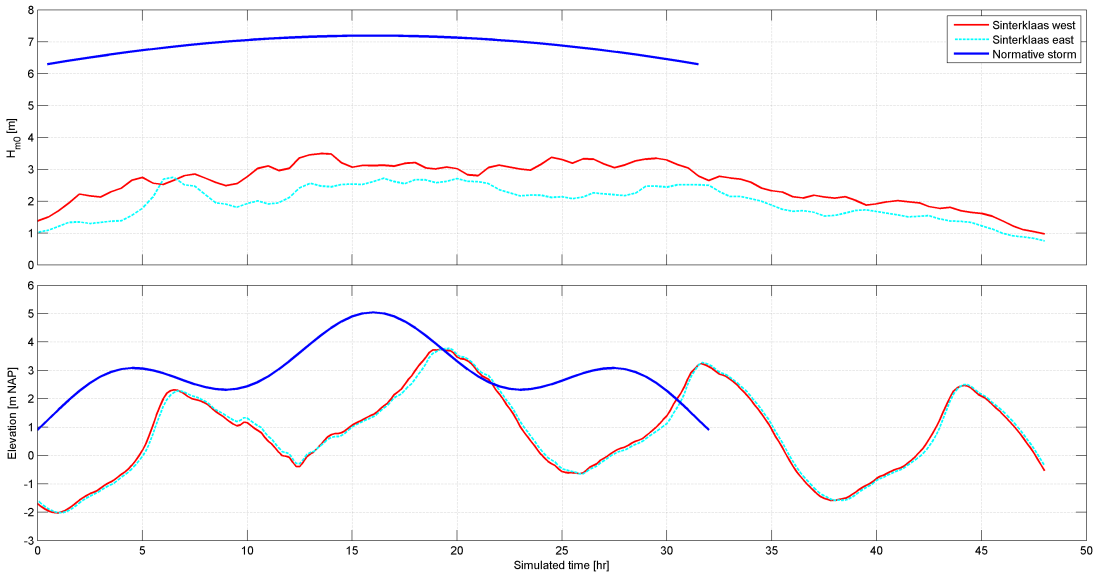

Figure 6.2: Hydrodynamic inputs for the normative storm.

The safety assessment against flooding in The Netherlands requires all component of the so-called ring dike (i.e. dikes, dunes, levees, etc.) to be able to cope with the hydraulic conditions associated to a return period of 10,000 years. Under this perspective, it is interesting to test the resistance of the dune field at Het Zwin to such storm.

The hydraulic conditions for this normative storm have been constructed following the hydrograms proposed by Vellinga (1986), and are presented in figure 6.2 along with the inputs used to model the Sinterklaas storm, for comparison. From the plots, it is clear that the normative storm is much severe than the 2013 storm; the water levels were more than one meter higher, extending the reach of the morphologically active areas, and the wave heights nearly doubled the record of the Sinterklaas event—meaning roughly four times more wave energy available for erosion and transport. Moreover, the hydrograms for the normative storm are explicitly constructed so that the maximum wave heights occur during the maximum water level, increasing their damaging potential.

The morphological impact of the normative storm is presented in figure 6.3. As expected, the predicted dune erosion is several times larger than observed during the Sinterklaas storm, particularly at the front of the dunes, which are heavily scarped at both sides of the runoff channel, which in turn seems to be strongly eroded by the ebb flow—in fact, the formation of a small ebb-tidal delta is observed below low water level, which was not present before.

The Dutch dunes once again experience overwash and deposition of sediment in their back-side, however this time the magnitude of the event is much larger, and actually these detached dunes tend to be almost completely eroded, and their sand reworked and redistributed in their vicinity. The overwash regime is only observed around the gap of this solitary dune row, whereas the rest of the dune field only experienced the collision regime.

Despite the high scale of destruction of the dunes under this scenario, the dikes surrounding Het Zwin would be only locally eroded in the sector right behind the mouth of the estuary. All other parts show little or no erosion at all, which is reassuring for the local communities and their safety.

It would appear that Het Zwin would withstand its normative storm, although it will likely lose the dunes that have been subject of this study. This might, in turn, make the dike behind them more vulnerable to following storm events.

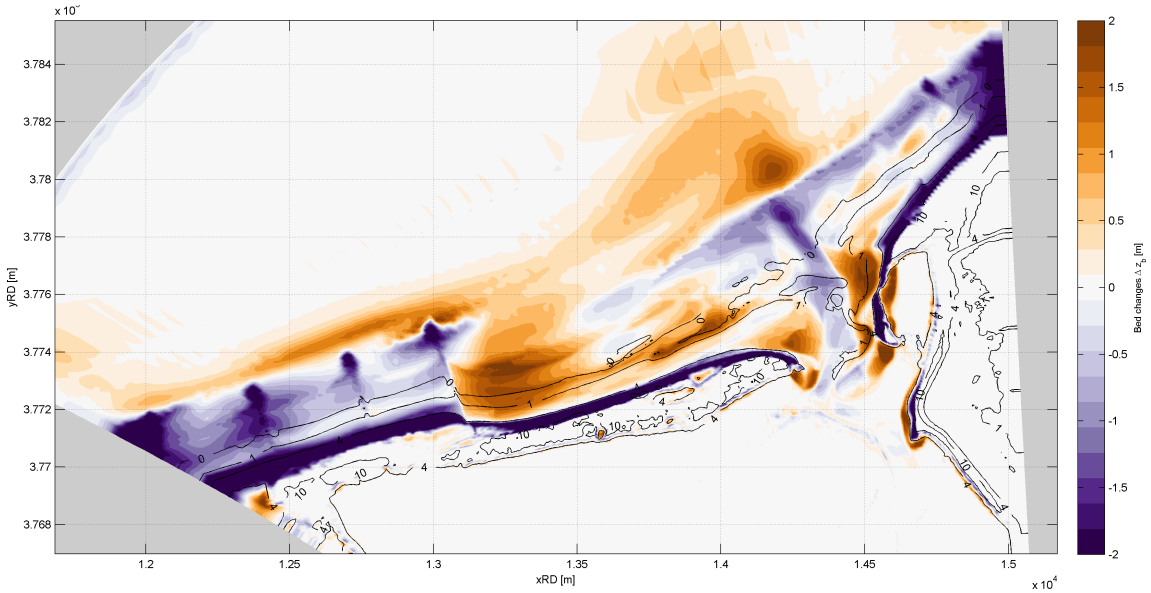

Figure 6.3: Morphological impact of the site's normative storm.

7

Discussion

7.1. Introduction

The previous chapters have focused on presenting the available data related to the Sinterklaas storm, their analysis to assess its impact on the dunes at Het Zwin, and the hind-cast of the storm using the numerical model XBeach, which required to test and apply model configurations that allowed the model to run in a workable time. Whenever decisions where taken or assumptions were made, they were simply stated or briefly argued for.

The objective of this chapter is to discuss some of the key assumptions used, and the questions that have arisen from this thesis work. Three subjects will be revised: the speed-up techniques presented and their possible expansions, a general comment on calibration methods, and a discussion of the effect of the morphological acceleration factor on the model's predictions.

7.2. Speed up techniques

It has been showed that it is possible to importantly reduce the runtime of XBeach by working out the grid configuration—first by choosing curvilinear grids over rectangular ones, and later by a straightforward offline coupling. However, it is also clear that the modeller must *need* to reduce this time in the first place. Without a proper incentive, it is tempting to stay in the comfort zone and keep using Cartesian grids, for which so many good and free tools are already available.

In this particular case, the incentive was the impossibility of using $f_{mor} > 1$, or to accelerate the model "from within", since the water level behind the dunes depended on the flow through the estuary gorge, which could not be accelerated to the same pace of the boundary conditions. In section 7.4 it will be argued that this is true for all modelling of overwash flow, regardless of the nature of the water level at the back-bay.

From a practical point of view, there are other options available to reduce the runtime: reducing the output size, increasing the CFL number, or even using a small `morfac`, say $f_{mor} = 2$. And of course, a combination of all the previous.

From the developer point of view, however, the goal of optimizing the runtime of XBeach seems to be closely related with the recent change in all Deltares software: the migration to a flexible mesh, which allows focusing on particular areas without involving the rest of the grid. Different areas, normally nested, are modelled as curvilinear grids with different resolutions, and are "glued" together with triangular grids that allow smooth transitions between them.

Moreover, this approach could allow different sub-models to run different sub-sets of physical processes, e.g. the sediment transport and avalanching should only take place in the grid covering the nearshore, which is a more sophisticated and robust way of achieving an online coupling between models. One

clear disadvantage of this approach would be the repetition of the offshore hydrodynamic computations across different runs, which was the main reason to opt for an offline coupling in this project.

7.3. Calibration method

Most hind-cast calibrations consist of a base run using the model's default settings, plus several other runs in which the most sensitive parameters of the model are varied—normally in a physically meaningful way—in order to find the set of parameters that most closely reproduce the observed phenomena.

The parameters to be calibrated normally have a large impact on the model results—otherwise they would not be used for calibration—however, a distinction should be made based on their nature, which is frequently overlooked or misstated in most calibration processes. At least three different categories of parameters should be regarded separately.

Physical parameters. These correspond to physical properties of the site or domain to be modelled. They could be thought as characteristics of the physical environment that could, in principle, be measured in situ. However, normally such a measurement is unavailable or challenging to be made at all, and the numerical model is used as a tool to estimate this parameter. A classical example is the Chezy or Manning coefficient to represent (steady) bottom friction.

Mathematical parameters. In this category lie the mathematical representations—and their specific parameters—of the physical processes. Rather than physical properties of the field, these parameters determine how the model will simulate the physical processes in a schematic way. A typical example can be the breaking of waves. Mathematical representations of this complex phenomenon can vary from the simplified saturation parameter γ_b up to turbulent simulation with a two phases fluid—which would employ several parameters.

Numerical parameters. These parameters are related with the discretization scheme rather than the physics of the model, and thus are often neglected from the calibration process. Typical examples are the grid resolution and the Courant number, which might influence greatly the model results since they determine the truncation error and hence the accuracy (and sometimes stability) of the model. For the particular case of XBeach, the accelerator factor, `morfac`, would lie in this category.

Based on this distinction, it could be argued that the calibrated parameters for bottom roughness `C` and onshore transport by short waves `facua` correspond to characteristics of the beach, and the modeller should try to make and educated guess on their values. Most of the times, the same model would be used to make a final estimation of these parameters, but it should be remarked that values obtained are not, necessarily, usable in other locations.

With respect to the calibration of mathematical parameters—like the breaking parametrization—they should, in principle, be validated within their own terms rather than in combination with several other process than might lead to non-physical values, i.e. the best set of parameters for every process to be modelled should be used from previous calibrations of those specific processes, and the use of different values should have founded reasons. For instance, one could imagine a storm impact model in which too much sand is being eroded by waves, as compared to the observed rates. One numerical solution would be to "calibrate" the breaking saturation parameter to a very small value, say $\gamma_b = 0.05$, which would clearly lie outside the range of observations for that parameter.

Keeping this distinction in mind, it has been decided to calibrate only the physical parameters in the hind-cast of the Sinterklaas storm, despite the fact that many mathematical parameters are known to be very sensitive on the results.

Finally, the improvement of accuracy due refinement of the numerical grid could also be considered as part of the calibration—in a sense, the model results start to be meaningful from a certain grid size. However, as shown in section 5.4, the runtime for very refined models tend to be excessive (the same applies for small Courant numbers), and hence the selection of a suitable grid normally remains within the "expert judgement" of the modeller.

Nonetheless, the question remains: are the calibrated physical parameters a function of these numerical parameters, in particular Δx and f_{mor}?

It could be argued that from a certain—small—grid size, the calibration should not depend on the spatial discretization, at least for most of the flow and waves computations. However, the avalanching algorithm relies on the model capability of assessing the slopes of the terrain, and hence it is strongly dependent on the grid resolution. This could be used as an argument for using milder critical slopes, since they don't need to necessarily correspond to the actual slopes on the beach, but rather with the slopes that the model is able to "observe".

The issue of the dependency of the calibrated parameters on the morphological accelerator factor will be discussed in the following section.

7.4. Morfac

Little discussion is available about the use of the morphological accelerator factor on XBeach. Most modellers indicate the use of a high value of the `morfac` parameter (normally 10) as a necessity to achieve workable runtimes, and normally this assumption is tested at some point in their reports in which "no significant differences were found" in the morphological results, hence justifying their decision.

Dissanayake *et al.* (2014) performed a sensitivity analysis of the use of the accelerator factor in their modelling of storm impact at Liverpool bay. They remark that larger volumes of sediments are lost from the domain when increasing the value of `morfac`, and determined that the best value for their hind-cast was not to use the accelerator factor (see figure 7.1). Their analysis gives insight on the behaviour of the accelerated model, but it is often prohibitive to perform. In other words, one would like to know beforehand which `morfac` is suitable to be used in a certain model.

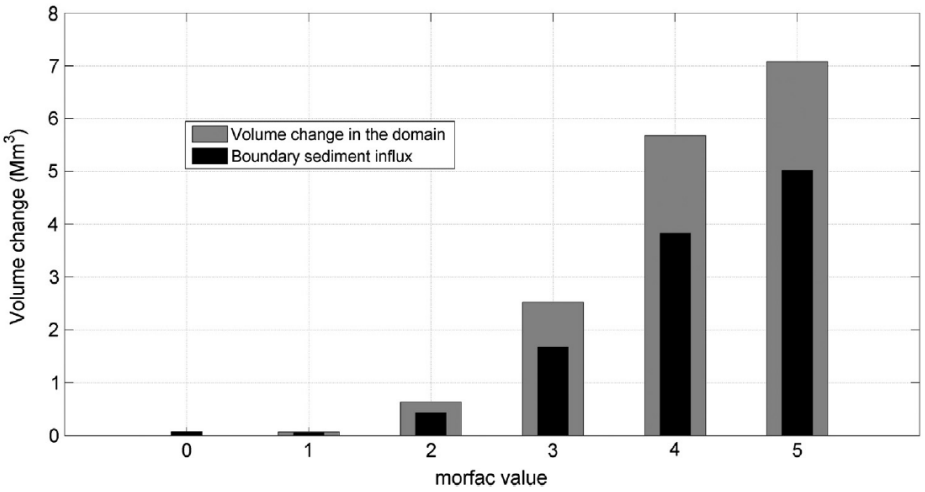

Figure 7.1: Mass conservation as a function of `morfac` in the work of Dissanayake *et al.* (2014).

Another interesting point was made by Ranasinghe *et al.* (2011), who suggested to compute a priori the maximum usable accelerator factor in long-term morphological simulations, as an analogy of the CFL condition, i.e. there must be a value of `morfac` for which the assumption of linearity of the morphological response is still reasonably valid. To the knowledge of the author, there is no such analysis for the morphological accelerator of XBeach, which differs in some regards with the "classical" factor.

In XBeach, the `morfac` parameter speeds up and deforms the water level signal used as input. Let this signal be $\eta(x,t)$, then the terms $\partial\eta/\partial x$ and $\partial\eta/\partial t$ are amplified by a factor equal to $f_{mor} = \texttt{morfac}$. Given the dimensions of most XBeach models, they tend to simulate the water level in pumping mode, i.e. the water level moves vertically without noticeable time lag across the domain, and hence the amplification of these terms in the boundary and at the coast and dunes should be similar.

The effect on the flow velocities, however, is less straightforward. Under collision regime this amplification apparently has no significant effect. In this case the beach acts like a closed basin, and the

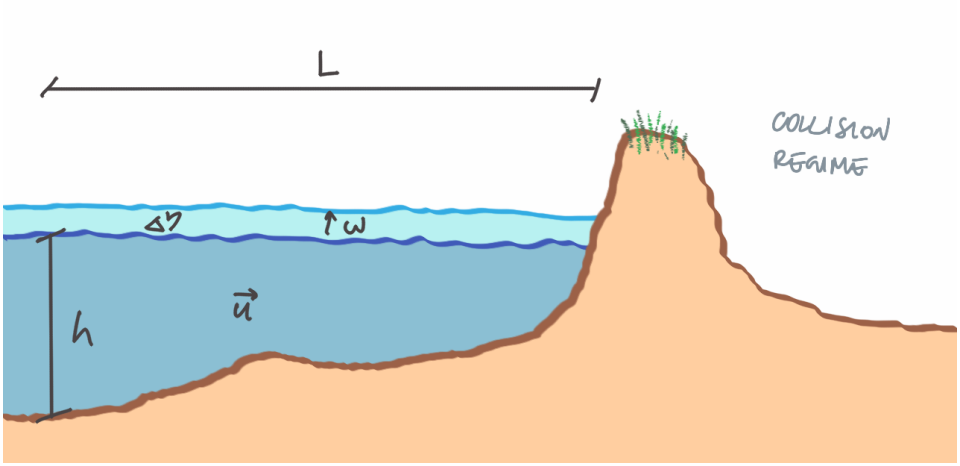

Figure 7.2: Effect of `morfac` over collision regime.

horizontal velocity u due to an increase of the water level will be (in a 1D case)

$$u = \frac{L}{h}\frac{\partial \eta}{\partial t} \cdot f_{mor} \tag{7.1}$$

where L is the length of the basin and h its mean depth (see figure 7.2). Using sensible values ($L \approx 1$ [km], $h \approx 10$ [m], $\Delta\eta \approx 5$ [m], $\Delta t = 6$ [hr]) the velocity with $f_{mor} = 1$ corresponds to $u = 0.02$ [m/s], and with $f_{mor} = 10$, to $u = 0.2$ [m/s], a tenfold difference. Nonetheless, both values are small enough as to not induce sediment transport, and hence the use of the accelerator factor under collision regime might well produce similar morphological results.

In a way, there is not really flow under this regime, and the physics-bending required to reduce the runtime of the model causes no harm.

By contrast, once the water is flowing over the dunes (or in a tidal channel, for that matter), the flow has its own time scale—governed by gravity—and the distortion of the water level signal begins to affect. Again in a 1D simplification, the dunes can be thought acting like a weir (see figure 7.3). Letting aside the short wave effects, mixing and Coriolis, the momentum equation for the horizontal velocity u would look like equation 7.2, meaning that the flow would accelerate under overwash or inundation regimes, in which the velocities are already high.

$$\frac{\mathbf{D}u}{\mathbf{D}t} = -g\frac{\partial \eta}{\partial x} \cdot f_{mor} - \frac{\tau_b}{\rho h} \tag{7.2}$$

It is normally argued that the velocity on top of the dunes during overwash is governed by the gradient of the water level at both side of the dunes, and since in many XBeach models both signals are modified by a factor `morfac` the modelled velocities are not affected. However, this reasoning is wrong, or at least incomplete.

Should the water flow inside a pipe, then the (stationary) velocity would be, in fact, determined solely by the gradient of the water levels. But the flow over the dunes under overwash and inundation regimes has an open-channel nature. Moreover, given the steep slopes on the back of the dunes it is very likely that the flow will be supercritical, and thus independent of the downstream conditions. The water level at the back bay, nonetheless, will determine the extension over which the water will flow, but the velocity of the flow will depend solely on the conditions at the top of the dune, and the use of a high `morfac` distorts these conditions.

This implies that a high `morfac` is likely to induce higher-than-real velocities under overwash regime, and given that sediment pick-up and transport are nonlinear functions of the flow velocity, they might be greatly overestimated in this regime.

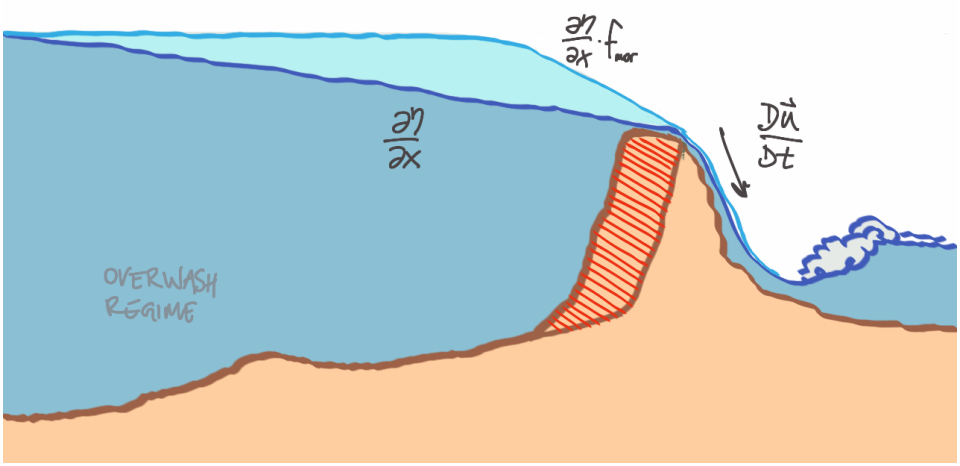

Figure 7.3: Effect of `morfac` over overwash regime.

Could this behaviour at least be one of the reasons why overwash is normally overestimated in XBeach simulations? The author finds this idea very plausible, although more research is needed to prove it fully.

Nonetheless, if that would be the case, what would imply for the calibration process? It seems likely that combinations of parameters that could hamper this larger-than-real erosion would be favoured, such as an ad-hoc `smax`, or physical properties of the beach like a high roughness and a high `facua` parameter (see section 2.4).

The idea that at least part of the calibrated values on previous studies is due to the distortions introduced by a high `morfac` seems likely, and the questions arises whether the same values would have been obtained should the model be run without acceleration.

As a test, the Zwin model was run with higher values of `morfac`, despite the fact that the tidal flow at the mouth is known to be badly modelled in this way. Figure 7.4 shows the computed impacts of the storm as a function of the accelerator factor, and is clear that very good agreement can be achieved for the overwash region, namely the extension and shape of the overwash fan and the scarping volumes, by tweaking the value of the onshore transport `facua`, which counteracts the amplification effect of a higher `morfac`. Of course, the rest of the domain is poorly modelled, especially the Belgian dunes which are under collision regimen, and should not be sensible to an acceleration of the water level input.

In short, the use of the accelerator factor in presence of flow, seems to create larger-than-real velocities, which in turn might induce excessive erosion. This could be one of the causes of the overestimation of XBeach during overwash regime. The calibration of the model under these conditions is not physically meaningful, since the hydrodynamics are heavily distorted, and the parameters obtained might not be representative of the site condition.

In the recent past, the use of the accelerator factor in XBeach has largely been taken for granted, since it allows to run the model in a reasonable time, but there is little published discussion about it. This thesis work is intended to shed light on that discussion, and at the very least, it has been proven that the use of a large `morfac` is not always required, nor the only way, to reduce the computing time on XBeach.

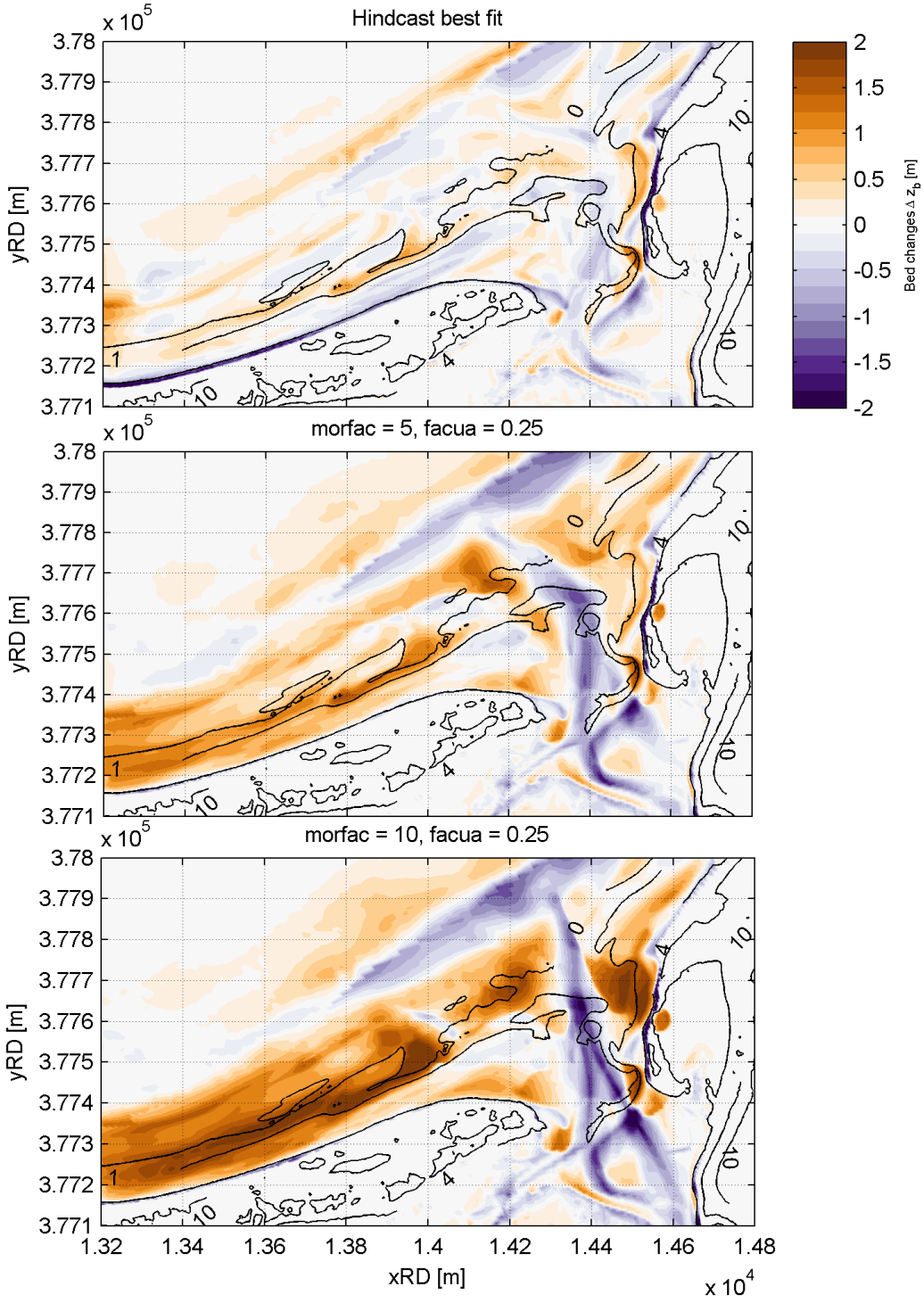

Figure 7.4: Sinterklaas at Het Zwin hind-cast for several values of `morfac`.

8

Conclusions and recommendations

8.1. Conclusions

In this thesis a hindcast of the morphological impact of the 2013 Sinterklaas storm at the tidal inlet of Het Zwin, in The Netherlands, has been carried out using the XBeach model. Topographic changes, as recorded by lidar measurements, indicate scarping of the dunes front at both sides of the tidal channel, and one location in the Dutch side where overwash occurred, hence comprising two distinguishable impact regimes—collision and overwash.

About the goodness of the hindcast, the following can be concluded:

- The agreement between the model and the measurements is very high. It can be stated that XBeach is able to reproduce collision and overwash regimes even in presence of a highly three-dimensional flow, as is the case in the tidal inlet.
- The overall trend of the changes in the topography is well represented, although there are some clear differences, especially on the deposition patterns along the tidal channel.
- Bottom friction (Chezy coefficient) is found to control the extension and shape of the overwash fan, whereas short wave induced onshore transport (`facua` parameter) and the critical slopes of avalanching are found to control the scarping process during collision regimen.
- The best fit for onshore transport by short waves was found with $\texttt{facua} = 0.1$, which is the default value on XBeach. This value is thought to be representative of the coast of Holland.
- The best fit for the bottom roughness was found with a Chezy coefficient of $C = 55$ in the deep bathymetry and the intertidal area, and a rougher value of $C = 25$ above the highest water level, estimated at 2.5 [m NAP] at Het Zwin.
- Both parameters, `C` and `facua`, are considered characteristics of the beach to be model, and thus rather than a the result of a model calibration, they are being estimated using the model. In other words, these correspond to model inputs rather than model parameters.
- An improvement on the volumes of eroded sand can be achieved in this case by lowering the critical slopes for avalanching. The best fit was obtained with $\texttt{wetslp} = 0.20$ and $\texttt{dryslp} = 0.85$, with the wet slope being the most sensitive parameter.
- These values are considered numerical parameters of the model, and not necessarily representative of the actual slopes on the terrain, since the effect of smoothing in the numerical grid might influence their choice.
- It was not necessary to use the numerical limiter `smax` to suppress excessive erosion and deposition in the overwash areas. In fact, the use of this limiter is not encouraged as it artificially hinders physical processes that might be better modelled with the use of other sensible physical parameters.

In order to produce simulations that would run in a workable time, an offline coupling scheme using curvilinear grids was adopted, which allowed to compute only once the hydrodynamic conditions in the deeper bathymetry of the domain, while focusing higher resolution in the dune fields.

Regarding the reduction of the runtimes of XBeach, the following can be concluded:

- The use of curvilinear grids instead of orthogonal ones can lead to substantial reduction of the computation times, while maintaining similar levels of accuracy. However, the production of curvilinear grids tends to be a time-consuming process.
- The offline coupling employed here—crude as it is—provides an accurate description of the oceanographic conditions at the nearshore which can be used as input for subsequent runs. This allows to separate the problem into one hydrodynamic part, run only once, and another morphodynamic part, which is run for as many combinations of parameters and conditions might be needed.
- The use of the morphological accelerator factor, `morfac` parameter, was not possible in this case, given the fact that the tidal flow through the mouth of the Zwin, and hence the water level behind the Dutch dunes, would not be correctly modelled.
- Moreover, even if it could be used, a high `morfac` value would induce larger-than-real velocities on top and in the back of the dunes under overwash regime. This might lead to overestimation of the dune erosion, and might be one of the causes of the historical overestimation of the washover fans and erosion volumes that XBeach has made for overash simulations.
- Historically, the main reason argued to use a high `morfac` is the reduction of the computation time. Since this can be achieved via other means, and given the fact that using the accelerator factor actually deforms the hydrodynamics with hard-to-foresee consequences, its use is not encouraged in overwash simulations.

8.2. Further research

The hindcast of the Sinterklaas storm at Het Zwin is considered a success, and the explored acceleration techniques are thought useful tools to improve the computational effort involved in modelling with XBeach. However, there are points to be addressed and questions to be asked, which will be proposed here for future researchers:

Sinterklaas hindcast. The main source of uncertainties for this case corresponds to the actual bathymetry at the beginning of the storm. The most recent lidar dataset was dated several months before the storm, and it is plausible it did not corresponded fully with the initial state of the beach.

One way to improve the hindcast would be to estimate the a corrected initial condition, most likely as the output of a long-term morphological simulation, for which all required data is available, i.e. wave parameters and water level records. The computations could be carried out with Delft3D or some other similar software, which might in turn require its own calibration, in order to produce a reliable bathymetry. The parameters to be calibrated and the methodology to do it are beyond the scope of this recommendation—they might include a measure of the improvement of the calibrated XBeach storm impact model—and should be defined as part of the research.

Acceleration of XBeach. The reduction in computation time by using curvilinear grids and decomposing the computations has been made evident in this thesis, and in previous works. These options rely on the modeller field of action, and are readily available with the current versions of XBeach. However, further improvement could be achieved by future developments of the model, among which the following can be counted (roughly sorted from easy to challenging changes):

- Optimizing the output for netCDF files. As it is today, the whole file with the output specifications is created and later filled up as the simulations advances, and this can easily lead to really large files. One common way around it is to determine a maximum file size, say 2 Gb, and to split the output in several smaller files containing the model results for the determined time intervals.

- Some kind of internal model separation—might be online coupling, model decomposition, etc.—which could allow to focus the morphodynamic computations in the area of interest, and not in the whole domain.
- The adoption of the flexible mesh approach. This would probably require the recoding of the whole software, but is very likely to improve dramatically the runtime of the model.

Morfac. It has been stated here that the use of a high `morfac` might be the cause of the historical overestimation of the overwash regime as modelled with XBeach, however this should be investigated further.

For instance, the hurricane impact modelled by de Vet *et al.* and Nederhoff *et al.* could be redo, now using `morfac` = 1 and improving the computation time as outlined here. It would be interesting to see if the observed morphological changes can be reproduced without the accelerator factor, and what would be the resulting calibrated parameters.

If a difference is observed, would that imply that part of the older set was counterbalancing the extra erosion caused by the large `morfac`? Or even before that, how to the hydrodynamic parameters compare? Is it true, in the first place, that they are exaggerated in the accelerated model?

Bibliography

A. H. Sallenger, Jr, *Storm impact scale for barrier islands,* Journal of Coastal Research **16**, 890 (2000).

P. Dissanayake, J. Brown, and H. Karunarathna, *Modelling storm-induced beach/dune evolution: Sefton coast, Liverpool Bay, UK,* Marine Geology **357**, 225 (2014).

Koninkijk Nederlands Meteorologisch Instituut, *Klimaatdata en advies. Zware storm op 5 december,* `http://www.knmi.nl/klimatologie/storm_dec13.html` (2013), accessed: 2015-Jan-22.

Hansa Luftbild/TopScan, *Kwaliteitsdocument laseraltimetrie. resultaten controles kust 2013,* (2013), (in Dutch).

Hansa Luftbild/TopScan, *Vluchtrapport. kust, sophiapolder en zandmotor 2014,* (2014), (in Dutch).

EUROSENSE, *LIDAR missie belgische kust – strand - voorjaar 2013,* (2013), (in Dutch).

EUROSENSE, *LIDAR missie belgische kust – extra vlucht strand - december 2013,* (2014), (in Dutch).

N. G. Plant, K. T. Holland, and J. A. Puleo, *Analysis of the scale of errors in nearshore bathymetric data,* Marine Geology **191**, 71 (2002).

N. G. Plant, K. L. Edwards, J. M. Kaihatu, J. Veeramony, L. Hsu, and K. T. Holland, *The effect of bathymetric filtering on nearshore process model results,* Coastal Engineering **56**, 484 (2009).

R. T. McCall, N. Plant, and J. van Thiel de Vries, *The effect of longshore topographic variation on overwash modelling,* in *Coastal Engineering*, 32 (2010).

R. B. van Santen, H. J. Steelzel, J. van Thiel de Vries, and A. van Dongeren, *Modelling storm impact on complex coastlines Westkapelle, The Netherlands,* in *Coastal Engineering*, 33 (2012).

F. Bisschop, P. Visser, C. van Rhee, and H. J. Verhagen, *Erosion due to high flow velocities: a description of relevant processes,* Coastal Engineering Proceedings **1**, sediment (2011).

R. T. McCall, J. S. M. van Thiel de Vries, N. G. Plant, A. R. Van Dongeren, J. A. Roelvink, D. M. Thompson, and A. J. H. M. Reniers, *Two-dimensional time dependent hurricane overwash and erosion modeling at santa rosa island,* Coastal Engineering **57**, 668 (2010b).

C. A. Lindemer, N. G. Plant, J. A. Puleo, D. M. Thompson, and T. V. Wamsley, *Numerical simulation of a low-lying barrier island's morphological response to hurricane katrina,* Coastal Engineering **57**, 985 (2010).

A. Terlouw, *Predicting morphological storm impact on coastal dunes at Ameland*, Master's thesis, University of Twente. Faculty of Engineering Technology. Department Water Engineering and Management (2013).

S. A. Stuij, *Process-based modelling of the Santo Andre Lagoon*, Master's thesis, Delft University of Technology. Faculty of Civil Engineering and Geocience. Department of Hydraulic Engineering. Programme of Coastal Engineering (2014).

P. L. M. de Vet, R. T. McCall, J. P. den Bieman, M. J. F. Stive, and M. van Ormondt, *Modelling dune erosion, overwash and breaching at Fire Island (NY) during hurrican Sandy,* in *Coastal Sediments 2015. San Diego, CA, USA, 11-15 May 2015* (2015) (accepted).

C. M. Nederhoff, Q. J. Lodder, M. Boers, J. P. den Bieman, and J. K. Miller, *Modeling the effects of hard structures on dune erosion and overwash,* in *Coastal Sediments 2015. San Diego, CA, USA, 11-15 May 2015* (2015) (accepted).

D. Roelvink, A. J. H. M. Reniers, A. R. van Dongeren, J. S. M. van Thiel de Vries, R. T. McCall, and J. Lescinski, *Modelling storm impacts on beaches, dunes and barrier islands,* Coastal Engineering **56**, 1133 (2009).

D. Roelvink, A. J. H. M. Reniers, A. R. van Dongeren, J. S. M. van Thiel de Vries, J. Lescinski, and R. T. McCall, *XBeach Model Description and Manual*, Unesco-IHE Institute for Water Education, Deltares and Delft University of Technology, 6th ed. (2010).

M. R. A. van Gent, J. S. M. van Thiel de Vries, E. M. Coeveld, J. H. de Vroeg, and J. van de Graaff, *Large-scale dune erosion tests to study the influence of wave periods,* Coastal Engineering **55**, 1041 (2008).

J. S. M. van Thiel de Vries, *Dune erosion during storm surges*, Ph.D. thesis, Delft University of Technology. Faculty of Civil Engineering and Geocience. Department of Hydraulic Engineering. Programme of Coastal Engineering (2009).

A. J. H. M. Reniers, J. A. Roelvink, and E. B. Thornton, *Morphodynamic modeling of an embayed beach under wave group forcing,* Journal of Geophysical Research: Oceans **109**, n/a (2004).

A. van Dongeren, A. J. H. M. Reniers, J. Battjes, and I. Svendsen, *Numerical modeling of infragravity wave response during DELILAH,* Journal of Geophysical Research: Oceans **108**, n/a (2003).

A. A. van Rooijen and J. S. M. van Thiel de Vries, *Stormgedreven morfodynamiek van De Slufter, Texel*, Tech. Rep. (Deltares, 2014) (in Dutch).

N. Wiegman, R. Perluka, S. Oude Elberink, and J. Vogelzang, *Vaklodingen: de inwintechnieken en hun combinaties. Vergelijking tussen verschillende inwintechnieken en de combinaties ervan. AGI-Rapport, AGI-2005-GSMH-012*, Tech. Rep. (Adviesdienst Geo-Informatica en ICT (AGI), 2005) (in Dutch).

D. Roelvink, G. Stelling, B. Hoonhout, J. Risandi, W. Jacobs, and D. Merli, *Development and field validation of a 2DH curvilinear storm impact model,* in *Coastal Engineering*, 33 (2012).

D. Roelvink, C. Den Heijer, and J. S. M. van Thiel de Vries, *Morphological modelling of strongly curved islands,* in *Coastal Dynamics 2013: 7th International Conference on Coastal Dynamics, Arcachon, France, 24-28 June 2013* (Bordeaux University, 2013).

P. van Geer, J. den Bieman, B. Hoonhout, and M. Boers, *XBeach 1D - Probabilistic model. ADIS, Settings, Model uncertainty and Graphical User Interface*, Tech. Rep. (Deltares, 2014) (preliminary).

J. Sutherland, A. H. Peet, and R. L. Soulsby, *Evaluating the performance of morphological models,* Coastal engineering **51**, 917 (2004).

J. Bosboom, A. J. H. M. Reniers, and A. P. Luijendijk, *On the perception of morphodynamic model skill,* Coastal Engineering **94**, 112 (2014).

P. Vellinga, *Beach and dune erosion during storm surges*, Ph.D. thesis, Delft University of Technology. Faculty of Civil Engineering and Geocience. Department of Hydraulic Engineering. Programme of Coastal Engineering (1986).

R. Ranasinghe, C. Swinkels, A. Luijendijk, D. Roelvink, J. Bosboom, M. Stive, and D. Walstra, *Morphodynamic upscaling with the MORFAC approach: Dependencies and sensitivities,* Coastal Engineering **58**, 806 (2011).